Cellular Sinoatrial Node and Atrioventricular Node Activity in the Heart

HJ Jansen and TA Quinn, Dalhousie University, Halifax, NS, Canada
RA Rose, Dalhousie University, Halifax, NS, Canada; University of Calgary, Calgary, AB, Canada

Introduction 1
Anatomy of the SAN and AVN 1
SAN and AVN Conduction 3
Sinoatrial Node Action Potentials 4
Atrioventricular Node Action Potentials 5
Ionic Basis for SAN APs 5
HCN channels 5
T-type and L-type calcium channels 6
Sarcoplasmic reticulum Ca^{2+} release and Na^{+}–Ca^{2+} exchange 6
Sustained inward current 7
Sodium channels 7
Inward rectifier potassium channels 7
Delayed rectifier potassium channels 7
Transient outward potassium channels 8
Two-pore potassium channels 8
Calcium-activated potassium channels 8
TRP channels 8
AVN Ion Channels 9
Regulation by the Autonomic Nervous System 10
Hormonal Regulation of the SAN by Natriuretic Peptides 11
Mechanical Effects on the SAN 11
Conclusions 12
References 13

Introduction

In order for blood to be delivered properly to the tissues of the body, the heart has to contract in an organized and coordinated fashion. The mammalian heart consists of both contractile (i.e., "working") cardiomyocytes (located in the atria and ventricles) as well as specialized pacemaker and conduction system cells that demonstrate automaticity (present at specific locations within the heart). The precise activity of the specialized cell types demonstrating automaticity in the heart results in the coordinated excitation of the contractile cardiomyocytes in the atria and ventricles, thereby ensuring proper pump function of the heart.

The components of the heart that demonstrate automaticity include the sinoatrial node (SAN), the atrioventricular node (AVN), and the His-Purkinje network (**Fig. 1**). Myocytes in each of these locations are capable of generating spontaneous action potentials (APs). Under normal conditions, the SAN demonstrates the highest rate of intrinsic spontaneous activity (and hence is normally the primary pacemaker of the heart). The AVN has a lower rate of intrinsic spontaneous activity and normally functions to transmit electrical signals (i.e., APs) from the atria to the ventricles. The His-Purkinje network, located in the ventricles, demonstrates the lowest rate of intrinsic spontaneous activity and is responsible for the rapid delivery of electrical signals to the working ventricular myocardium. Abnormal activity in any of these specialized components of the heart can result in cardiac arrhythmia.

Anatomy of the SAN and AVN

The SAN is a small, condensed area of tissue located subendocardially, adjacent to the cristae terminalis, and within the intercaval region of the right atrium (Keith and Flack, 1907; Boyett et al., 2003; Dobrzynski et al., 2007; Mangoni and Nargeot, 2008; Liu et al., 2007) (**Fig. 1**). Developmentally, the SAN and AVN are formed from specific populations of progenitor cells and are regulated by specific transcriptional pathways that result in the specification and differentiation of the SAN and AVN. The reader is referred to excellent reviews on the topic of patterning of the SAN and cardiac conduction system for additional information on these topics (Christoffels et al., 2010; van Weerd and Christoffels, 2016; Vedantham, 2015).

SAN myocytes are smaller than atrial myocytes and exist in a number of morphologies including spindle shaped, elongated spindle shaped, or spider cells (Anderson et al., 2009; Boyett et al., 2000; Mangoni and Nargeot, 2001). The SAN is a heterogeneous structure that can be divided into the SAN center, which most frequently contains the leading pacemaker site, and SAN periphery

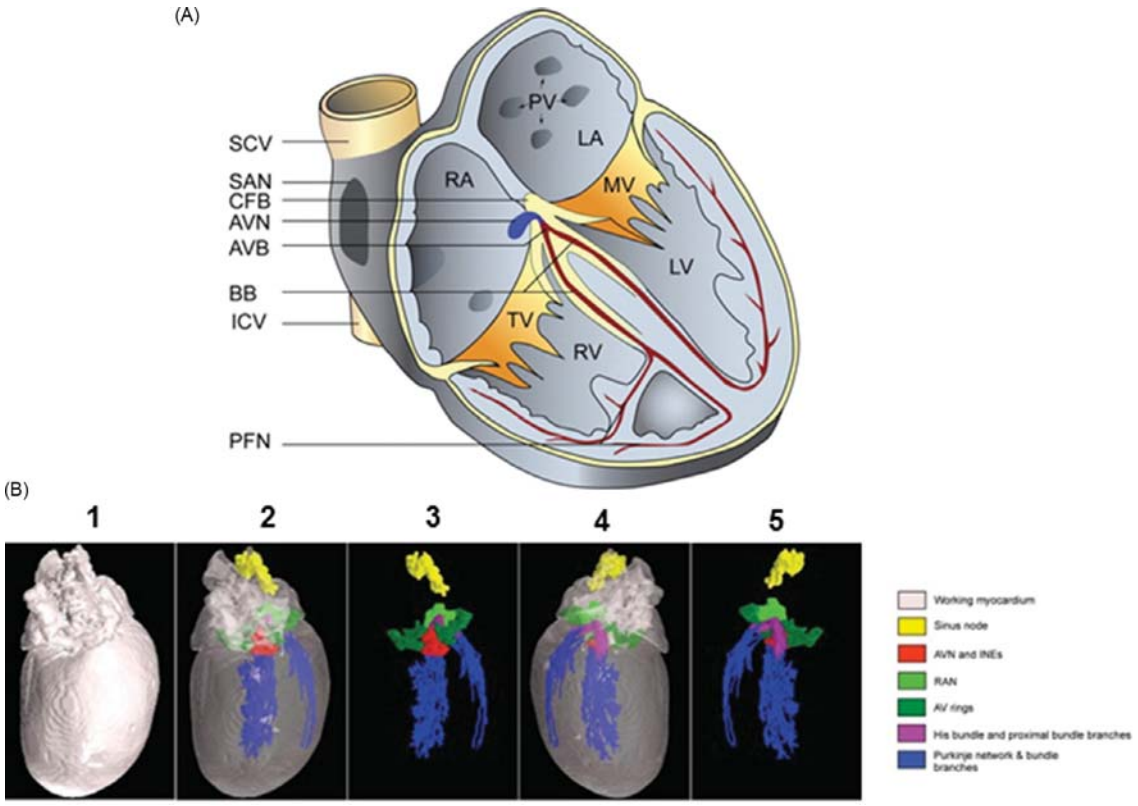

Fig. 1 (A) Schematic illustration of the heart showing the location of the sinoatrial node (SAN) and the components of the cardiac conduction system including the atrioventricular node (AVN), the atrioventricular bundle (AVB), the bundle branches (BB), and the Purkinje fiber network (PFN). LA, left atrium; RA, right atrium; SCV, superior vena cava; IVC, inferior vena cava; CFB, central fibrous body; PV, pulmonary vein; TV, tricuspid valve; MV, mitral valve; RV, right ventricle; LV, left ventricle. (B) The three-dimensional model of the SAN and cardiac conduction system including (1) a model of the heart from the dorsal epicardial surface, (2) a transparent model of the heart with a view of the sinoatrial node and cardiac conduction system from the dorsal surface, (3) a model of the SAN and cardiac conduction system in isolation as viewed from the dorsal surface, (4) a transparent model of the heart with a view of the sinoatrial node and cardiac conduction system from the ventral surface, and (5) a model of the SAN and cardiac conduction system in isolation as viewed from the ventral surface. (A) Reproduced with permission (Mangoni, M. E. and Nargeot, J. (2008). Genesis and regulation of the heart automaticity. Physiological Reviews 88, 919–982). (B) Modified and reproduced with permission (Atkinson, A.J., Logantha, S.J., Hao, G., Yanni, J., Fedorenko, O., Sinha, A., Gilbert, S.H., Benson, A.P., Buckley, D.L., Anderson, R.H., Boyett, M.R. and Dobrzynski, H. (2013). Functional, anatomical, and molecular investigation of the cardiac conduction system and arrhythmogenic atrioventricular ring tissue in the rat heart. Journal of the American Heart Association 2, e000246).

(Dobrzynski et al., 2007). SAN myocytes in the center are smaller compared with those in the periphery, and have distinct molecular and electrophysiological properties that will be discussed further throughout this chapter.

There is considerable variability in the structure of the SAN between different species. In the human and canine heart, the SAN is commonly "cigar shaped" with the head located lateral to the crista terminalis near the opening of the superior vena cava and a tail that extends toward the opening of the inferior vena cava to varying extents. In the rabbit heart, the SAN spans the region between the superior and inferior vena cava (Inada et al., 2014). In contrast, the mouse SAN is "comma shaped," with a dense region at the top of the comma near the superior vena cava and a tail that runs adjacent to the cristae terminalis (Liu et al., 2007). SAN myocytes are interspersed within a network of connective tissue that serves as an insulator (Opthof, 1988; Dobrzynski et al., 2007; Boyett et al., 2003; Chandler et al., 2009). This connective tissue, along with the SAN arteries and adipose tissue, insulate the SAN from the surrounding atrial myocardium (Fedorov et al., 2009, 2012). The mouse SAN contains relatively low levels of connective tissue and has finger-like projections that are one to three cells long and one to two cells wide, which extend into the surrounding atrial myocardium to a length of $\sim$200 μm (Liu et al., 2007).

The anatomy of the AVN was first detailed in 1906, where Sunao Tawara meticulously detailed the cardiac conduction system in various mammals, including humans (Tawara, 2000). The AVN is often separated into two regions including the compact node and the lower nodal bundle (**Fig. 2**). The compact node is a half-oval shaped, small, dense region of interweaving spindle-shaped cells situated at the apex of the triangle of Koch adjacent to the central fibrous body (Hucker et al., 2008; Dobrzynski et al., 2013; Meijler and Janse, 1988; Inoue and Becker, 1998; Anderson and Ho, 1998). Morphologically, cells within the compact node are small and spindle or ovoid shaped (Munk et al., 1996). The anterior portion of the AVN is occupied by the lower nodal bundle and includes the rightward inferior nodal extension (INE). INEs are regions of specialized tissue that extend from the coronary sinus ostium and

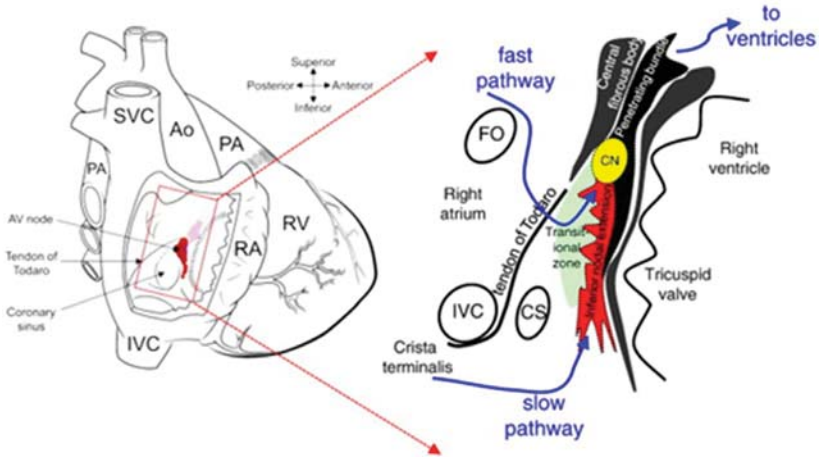

Fig. 2 Location of the atrioventricular node within the heart (left) and schematic illustration of the atrioventricular node junction including the fast and slow pathways (right). Ao, aorta; CN, compact node; CS, coronary sinus; FO, fossa ovalis; IVC, inferior vena cava; SVC, superior vena cava; RA, right atrium; RV, right ventricle. Reproduced with permission from Dobrzynski, H., Anderson, R.H., Atkinson, A., Borbas, Z., D'Souza, A., Fraser, J.F., Inada, S., Logantha, S. J., Monfredi, O., Morris, G.M., Moorman, A.F., Nikolaidou, T., Schneider, H., Szuts, V., Temple, I. P., Yanni, J. and Boyett, M.R. (2013). Structure, function and clinical relevance of the cardiac conduction system, including the atrioventricular ring and outflow tract tissues. Pharmacology and Therapeutics 139, 260–288.

are continuous with the compact node, which have been identified in the dog and human heart (Hucker et al., 2008; Inoue and Becker, 1998; Anderson and Ho, 1998). Cells located in this region are smaller than atrial myocytes, yet larger than those in the compact node. They are tightly packed and organized in a parallel configuration. Surrounding the compact node and INE are transitional cells. These cells have a unique cellular phenotype as they exhibit morphological and electrophysiological characteristics of cells within the compact node as well as the surrounding myocardium in which they are located (Anderson and Latham, 1971; Anderson et al., 1974; Temple et al., 2013; Efimov et al., 2004). Electrophysiology studies have identified three cell types within the AVN including the atrio-nodal, the nodal, and the nodo-his cells (Nikolaidou et al., 2012).

SAN and AVN Conduction

In the intact SAN, the leading pacemaker site is the location of initial breakthrough of electrical activity and is most commonly located within the intercaval region (Dobrzynski et al., 2007; Mangoni and Nargeot, 2008). It is estimated that the leading pacemaker site accounts for roughly 1% (approximately 5000 cells) of the SAN in the rabbit heart (Bleeker et al., 1980; Kodama and Boyett, 1985). In response to physiological and pathophysiological conditions, the location of the leading pacemaker site can change. For example, a superior shift occurs in response to sympathetic nervous system activation with β-adrenergic receptor (β-AR) agonists (Fedorov et al., 2012; Azer et al., 2014). Similarly, activation of the parasympathetic nervous system or application of muscarinic (M_2) agonists produces an inferior shift in leading pacemaker site (Fedorov et al., 2012; Vinogradova et al., 1998; Krishnaswamy et al., 2015). Circulating hormones, such as natriuretic peptides (NP), can also modulate SAN function in association with shifts in leading pacemaker site (Azer et al., 2014). Furthermore, in the aged mouse heart it has been shown that the location of the leading pacemaker site can alternate between a superior and inferior position in subsequent beats and change as a function of frailty (Moghtadaei et al., 2016a). It has been proposed that these shifts in leading pacemaker site alter heart rate because of different properties of SAN myocytes at the different locations within the SAN.

Conduction across the SAN spreads from the leading pacemaker site toward the periphery of the SAN at the cristae terminalis where it excites the surrounding atrial myocardium. Interestingly, there is a band of nonexcitable tissue, commonly referred to as a "block zone," at the periphery of the SAN, which slows or prevents conduction toward the left atrium (Boyett et al., 2000, 2003; Bleeker et al., 1980; Nikolaidou et al., 2012). Myocytes at the center of the SAN exhibit poor electrical coupling, which has been attributed to cell orientation, increased levels of connective tissue, and gap junction protein expression patterns (Boyett et al., 2000, 2003; Dobrzynski et al., 2007; Chandler et al., 2009).

Connexins (Cxs) are critical proteins in the SAN (and AVN) that facilitate the spread of electrical signals between adjacent cells via gap junctions and are expressed heterogeneously in the SAN (and atria). The center of the SAN expresses the low conductance Cx45, but lacks expression of Cx40 and Cx43 (Boyett et al., 2000; Coppen et al., 1999; Verheijck et al., 2001). In the SAN periphery, both Cx43 and Cx45 are expressed, resulting in both an increase in electrical coupling between myocytes and increased conduction velocity (Coppen et al., 1999; Verheijck et al., 2001). Heterogeneity in Cx expression results in a slower conduction velocity within the SAN center compared with the periphery as well as the surrounding atrial myocardium and contributes to protecting the SAN from the hyperpolarized atrial myocardium (Joyner and van Capelle, 1986; Boyett et al., 2000; Mangoni and Nargeot, 2008; Bartos

et al., 2015). Cxs are also critical for the activation of the atria by the SAN whereby the coupling of Cx45 expressing regions of the SAN communicate with Cx40 and Cx43 positive regions of the atria (Verheijck et al., 2001). It has been proposed that the SAN communicates with the surrounding atrial myocardium via distinct exit pathways in the SAN (Fedorov et al., 2012; Csepe et al., 2016).

The AVN serves as a gateway to the ventricles as APs generated in the atria must pass through the AVN to excite the ventricular myocardium. Conduction throughout the AVN is much slower than the atria, which has been attributed to numerous factors including cell orientation, intracellular coupling, and ion channel expression. In larger animals, including humans, two distinct pathways of conduction through the AVN have been identified based on electrophysiological characteristics and molecular properties. These are referred to as the fast and slow pathways because of the ease with which conduction spreads through each, which is correlated with Cx43 expression (Hucker et al., 2008; Kurian et al., 2010; Temple et al., 2013). The fast pathway demonstrates relatively rapid conduction velocity, a long refractory period, and has very little to no Cx43 expression. This pathway includes the transitional cells, leftward INE, and compact node (Temple et al., 2013; Hucker et al., 2008; Greener et al., 2011; Efimov et al., 2004; Mani and Pavri, 2014). In contrast, Cx43 is expressed throughout the slow pathway (Cx43 positive region), which includes the rightward INE and the lower nodal bundle, and is continuous with the His bundle (Hucker et al., 2008). As the name suggests, conduction velocities are slow in this pathway (Mani and Pavri, 2014).

Sinoatrial Node Action Potentials

The quintessential feature of the SAN is its ability to generate spontaneous APs characterized by the presence of a slow diastolic depolarization (DD) between successive APs (**Fig. 3A**). The DD occurs during diastole and is characterized by a gradual increase in resting membrane potential, starting from the maximum diastolic potential (MDP) until the threshold for the next AP is reached (DiFrancesco, 1993; Irisawa et al., 1993). In SAN myocytes the AP upstroke velocity (V_{max}) is slower, the overshoot (OS) is smaller, and AP duration (APD) is longer compared to the surrounding contractile atrial myocytes (Monfredi et al., 2010; Dobrzynski et al., 2007). AP morphology is also heterogeneous within the SAN from center to periphery (**Fig. 3B**). Using small ball preparations of consecutive regions within the SAN, intrinsic differences in AP morphology have been characterized. Specifically, from the periphery to the center of the SAN, there is a gradual decrease in AP V_{max}, OS, and MDP (Kodama and Boyett, 1985; Kodama et al., 1997; Boyett et al., 1999). Furthermore, there is an increase in APD from the periphery toward the center of the SAN (Kodama et al., 1997; Yamamoto et al., 1998; Boyett et al., 1999).

Morphologically, APs recorded from the periphery of the SAN have some resemblance to atrial APs while still retaining properties of spontaneously active SAN myocytes (Yamamoto et al., 1998) (**Fig. 3B**). For example, peripheral SAN myocytes have a prominent DD and display automaticity; however, V_{max} is faster and APD is shorter in peripheral versus central SAN myocytes (Boyett et al., 1999; Dobrzynski et al., 2007). Collectively, these AP differences across the SAN result in the leading pacemaker site depolarizing first, but repolarizing last (Yamamoto et al., 1998; Boyett et al., 2000). This is of functional importance because it prevents re-entrant activity.

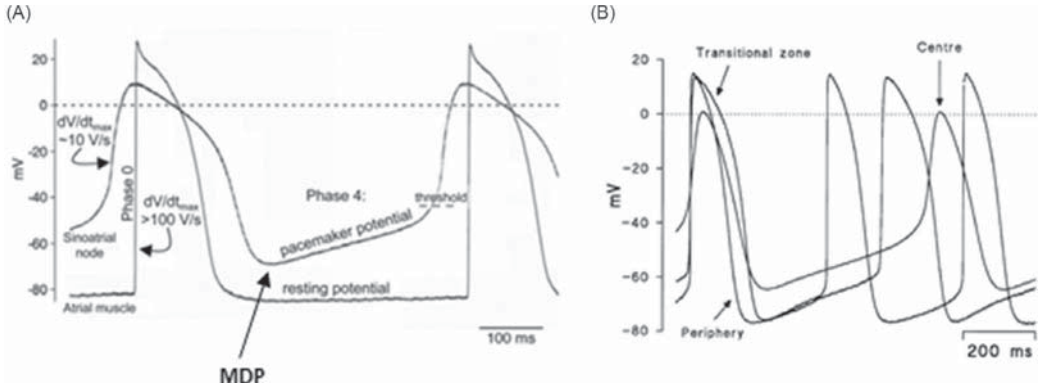

Fig. 3 Action potential morphologies in the sinoatrial node and atrial myocardium. (A) Overlay of representative action potentials from the working atrial myocardium and the sinoatrial node. In comparison to atrial muscle, sinoatrial node action potentials are characterized by a depolarized MDP, a diastolic depolarization (DD; also referred to as a "pacemaker potential"), a reduced upstroke velocity (V_{max}, dV/dt_{max}), lower action potential amplitude and longer action potential duration. (B) Heterogeneity in spontaneous action potential morphology in the center, transitional zone, and periphery of the sinoatrial node. (A) Modified and reproduced with permission from Boyett, M. R. (2009). "And the beat goes on." The cardiac conduction system: The wiring system of the heart. Experimental Physiology 94, 1035–1049. (B) Reproduced with permission from Boyett, M.R., Honjo, H., Yamamoto, M., Nikmaram, M.R., Niwa, R. and Kodama, I. (1999). Downward gradient in action potential duration along conduction path in and around the sinoatrial node. The American Journal of Physiology 276, H686–H98.

Atrioventricular Node Action Potentials

APs within the AVN are unique compared with other regions in the heart. Specifically, AVN myocytes generate spontaneous APs that are characterized by much lower V_{max} values compared to the working myocardium. Furthermore, APs in AVN myocytes are shorter in duration compared with ventricular myocytes, but not atrial myocytes (Munk et al., 1996). While AVN myocytes are spontaneously active, their APs are characterized by slower spontaneous beating rates, reduced DD slopes, more negative MDPs, and reduced AP thresholds compared with SAN myocytes (Marger et al., 2011b).

Regional differences in AP morphology have been characterized in atrio-nodal cells (rod-shaped cells) and compact node or nodo-his cells (ovoid cells) isolated from the rabbit heart. Compact AVN cells are characterized by the presence of a rounded AP OS (Munk et al., 1996). Furthermore, these compact AVN cells have the lowest V_{max}, OS, APD, and MDP compared with the other regions of the AVN (Munk et al., 1996). In contrast, AP morphology of atrio-nodal cells demonstrates characteristics of both AVN and atrial myocytes (Munk et al., 1996; Yuill and Hancox, 2002).

Ionic Basis for SAN APs

The unique morphology of the SAN AP comes about due to the activities of a number of underlying ionic currents in SAN myocytes. These include the hyperpolarization-activated current (I_f) carried by hyperpolarization-activated cyclic-nucleotide gated (HCN) channels, T- and L-type Ca^{2+} currents, a number of voltage-dependent K^+ currents, a sustained inward current (I_{st}), and a Na^+–Ca^{2+} exchange (NCX) current (I_{NCX}) driven by the release of Ca^{2+} from the sarcoplasmic reticulum (SR) (Mangoni and Nargeot, 2008; Lakatta et al., 2010). Other currents and ion channels that have been shown to affect SAN AP firing include sodium channels, two pore K^+ channels, inward rectifier K^+ channels, Ca^{2+} activated K^+ channels, transient receptor potential (TRP) channels, and stretch-activated ion channels. A terminology that has seen widespread adoption is that ionic currents across the plasma membrane that affect SAN AP potential firing may be collectively referred to as a "membrane clock," while the SR Ca^{2+} release/I_{NCX} mechanism may be referred to as the "Ca^{2+} clock" (Lakatta et al., 2010). There has been considerable debate regarding whether any one ionic mechanism is essential for automaticity (i.e., generation of the DD) and regarding the relative importance of each of the ionic mechanisms that underlie spontaneous activity in the SAN (Lakatta and DiFrancesco, 2009). There is currently no consensus on these issues; however, when considered collectively, it appears that there is some redundancy in the ionic mechanisms that generate the DD and automaticity in the SAN.

HCN channels

The hyperpolarization-activated current, also known as the "funny" current (I_f), is encoded by HCN channels and contributes to the DD phase of the AP. Multiple HCN isoforms are expressed in the heart, including HCN1–4. HCN4 is thought to be the predominant isoform in the SAN with contributions from HCN1 and HCN2 as well. Functionally, HCN isoforms assemble into heteromultimeric complexes and the resulting I_f current has biophysical properties consistent with this structural arrangement (Monfredi et al., 2010; Accili et al., 2002; Bucchi et al., 2012). In many species, including mouse, rabbit, and dog, HCN4 expression accounts for upward of 80% of the total HCN expression in the SAN (Shi et al., 1999; Zicha et al., 2005; Liu et al., 2007). However, in the human SAN, HCN1 is highly expressed in addition to HCN2 and HCN4 (Chandler et al., 2009; Li et al., 2015).

As their name suggests, HCN channels are activated by hyperpolarization of the membrane potential and play a role in the early phase of DD (Baruscotti et al., 2010; DiFrancesco and Borer, 2007). I_f channels conduct both Na^+ and K^+, are blocked by Cs^+ in a voltage-dependent fashion, have a reversal potential between −10 and −20 mV, and exhibit slow activation and deactivation kinetics (Baruscotti et al., 2010; DiFrancesco and Borer, 2007; Accili et al., 2002). Inside-out patch-clamp experiments have shown direct activation of I_f channels by cAMP (i.e., independently of protein kinase A (PKA) phosphorylation); therefore, these channels are activated by both membrane voltage and cAMP (DiFrancesco and Tortora, 1991; Wainger et al., 2001). Physiologically, these effects allow for cAMP-dependent regulation of I_f channels, which functions to shift the voltage dependence of activation of HCN channels, increasing I_f currents and DD slope in SAN myocytes. In isolated rabbit SAN myocytes, 2 mM Cs^+ almost completely blocks I_f (Denyer and Brown, 1990). Interestingly, the same concentration of Cs^+ slows AP firing frequency by ∼30% rather than causing a complete cessation of AP firing. Similarly, in isolated rabbit SAN myocytes, ivabradine, a selective I_f blocker, reduced the spontaneous beating rate by 16%, which was attributed to a 32% reduction in early DD slope (Bucchi et al., 2007). Similar effects of Cs^+ on I_f and AP firing have been reported in the human heart (Verkerk et al., 2007).

Strong evidence of a role for I_f in the SAN, as well as the involvement of specific ion channel isoforms in its generation, comes from studies using genetically modified mice. For example, HCN1 knockout mice display a significant reduction (∼30%) in I_f density and spontaneous AP firing frequency in isolated SAN myocytes (Fenske et al., 2013). Furthermore, HCN1 knockout mice are characterized by bradycardia, impaired SAN conduction, and sinus pauses in vivo. Collectively, these findings confirm that HCN1 is present in the SAN and contributes functionally to I_f current generation.

Genetic deletion of HCN2 channels also results in a reduction in I_f density (∼30%) in isolated SAN myocytes as well as a slowing of I_f activation, indicating that HCN2 contributes to I_f in the mouse SAN (Ludwig et al., 2003). HCN2 knockout mice do not show a change in heart rate, but they are characterized by enhanced SAN-mediated arrhythmias, suggesting that HCN2 is important for normal SAN function.

Consistent with the hypothesis that HCN4 is the major isoform in the SAN, global deletion of HCN4 is embryonic lethal; embryos lacking HCN4 die by day 12 post coitum (Stieber et al., 2003). Prior to day 12 HCN4 knockout embryos show near

complete absence of I_f and slow heart rates (Stieber et al., 2003). The impacts of inducible and tissue-specific HCN4 ablation have also been investigated. In one study, Cre-lox methods were used to delete HCN4 from the adult mouse SAN, which reduced I_f by ~75% (Herrmann et al., 2007). Isolated SAN cells from these mice displayed irregular patterns of AP firing, but this could be restored to normal upon application of isoproterenol (ISO), indicating that the cells were capable of beating spontaneously despite the loss of I_f. The authors concluded that HCN4 was necessary for stable basal automaticity, especially at low heart rates (Herrmann et al., 2007). A second study that investigated inducible, cardiac-specific deletion of HCN4 in mice reported a more severe phenotype in which mice were characterized by severe bradycardia, as well as AV node block, ultimately resulting in death within 5 days of deletion (Baruscotti et al., 2011). Isolated SAN myocytes from these mice exhibited reductions in I_f of ~70%, while spontaneous AP firing was reduced by 60%. Taken together, the available data clearly demonstrate that I_f is importantly involved in generating automaticity in the SAN, although there is still continued debate on whether it is essential for this function.

T-type and L-type calcium channels

Voltage-gated calcium channels are expressed in the SAN and contribute to the DD in SAN myocytes (Mangoni et al., 2006a; Marionneau et al., 2005). In the heart, L-type calcium current ($I_{Ca,L}$) is encoded by two subunits, $Ca_V1.2$ and $Ca_V1.3$, while the T-type calcium current ($I_{Ca,T}$) is encoded by the subunits $Ca_V3.1$, $Ca_V3.2$, and $Ca_V3.3$ (Marionneau et al., 2005). These α subunits show distinct patterns of expression in different parts of the heart, as noted later.

With regard to $I_{Ca,L}$ channel expression, studies have revealed that $Ca_V1.2$ is expressed through the myocardium including in the SAN, while $Ca_V1.3$ has a more restricted expression pattern, being present in the SAN, AVN, and atrial myocardium, but absent from the ventricular myocardium (Mangoni et al., 2003). Functionally, $Ca_V1.3$-mediated $I_{Ca,L}$ is activated at more negative membrane potentials (compared with $Ca_V1.2$-mediated $I_{Ca,L}$), which correspond to membrane voltages during the DD (Mangoni et al., 2003; Mesirca et al., 2016b). $Ca_V1.2$, on the other hand, is primarily active during the AP upstroke. Bradycardia is observed in $Ca_V1.3$-deficient mice, which is attributed to a significant increase in the cycle length between successive APs in association with a reduction in the slope of the DD (Mangoni et al., 2003; Torrente et al., 2016). $Ca_V1.3$-deficient mice display a 60%–70% reduction in $I_{Ca,L}$ density and a positive shift in $I_{Ca,L}$ activation kinetics in SAN myocytes consistent with the remaining $I_{Ca,L}$ being generated by $Ca_V1.2$ (Mangoni et al., 2003). Combined, these data indicate $Ca_V1.3$-mediated $I_{Ca,L}$ contributes importantly to SAN pacemaker activity during the late phase of the DD and that this is the predominant L-type Ca^{2+} channel contributing to automaticity. $Ca_V1.2$-mediated $I_{Ca,L}$, while contributing importantly to the generation of the AP upstroke, does not appear to be a major participant in the generation of the DD.

For $I_{Ca,T}$, both $Ca_V3.1$ and $Ca_V3.2$ mRNAs have been found in the SAN; however, $Ca_V3.1$-mediated $I_{Ca,T}$ appears to play a more prominent functional role (Mesirca et al., 2014; Mangoni and Nargeot, 2008). $I_{Ca,T}$ demonstrates slower activation kinetics and accelerated inactivation kinetics compared with $I_{Ca,L}$ (Mesirca et al., 2014; Mangoni and Nargeot, 2008). Furthermore, $I_{Ca,T}$ activates at more negative membrane potentials than $Ca_V1.2$- and $Ca_V1.3$-mediated $I_{Ca,L}$ and the peak $I_{Ca,T}$ density is lower than that of $I_{Ca,L}$ in SAN myocytes. Nevertheless, $Ca_V3.1$-mediated $I_{Ca,T}$ has been shown to contribute to pacemaker activity in the SAN. Specifically, mice lacking $Ca_V3.1$ completely lack detectable $I_{Ca,T}$ in SAN myocytes, which resulted in a 37% reduction in spontaneous AP firing frequency (Mangoni et al., 2006b). Functionally, while basal heart rate was unchanged in $Ca_V3.1$ knockout mice, intrinsic heart rate (measured in the presence of autonomic nervous system blockade) was reduced by 10%. The precise mechanisms by which $I_{Ca,T}$ affects the DD are still unclear, but may involve the generation of a window current or the coupling of $I_{Ca,T}$ to intracellular Ca^{2+} handling.

Sarcoplasmic reticulum Ca^{2+} release and Na^+–Ca^{2+} exchange

Evidence of a role for sarcoplasmic reticulum (SR) Ca^{2+} release in cardiac automaticity was first shown in latent pacemaker cells in the atria and in the SAN, whereby application of ryanodine was found to slow spontaneous pacemaker activity (Rubenstein and Lipsius, 1989; Rigg and Terrar, 1996; Li et al., 1997). Since then, this phenomenon has been explored in great detail in the mammalian SAN (Lakatta et al., 2010). The central tenet of this hypothesis is that localized subsarcolemmal Ca^{2+} release (LCR) events from the SR occur during the late DD. These LCRs occur rhythmically and lead to the activation of NCX, which extrudes this Ca^{2+} from the SAN myocytes, thereby generating an inward current (I_{NCX}) during the DD. This SR Ca^{2+} release/I_{NCX} mechanism appears to depend on a high level of basal PKA activity in the SAN and is controlled by phosphodiesterases, which are responsible for hydrolyzing cAMP (Vinogradova et al., 2006, 2008). It has been proposed that the LCR events present during the DD occur spontaneously and do not depend on membrane depolarization (Lakatta et al., 2010). On the other hand, more recent evidence has demonstrated that $Ca_V1.3$ Ca^{2+} channels are colocalized with ryanodine receptors in the SAN (Christel et al., 2012) and it has been suggested that Ca^{2+} influx via $Ca_V1.3$ channels during the DD may lead to the opening of ryanodine receptors by Ca^{2+}-induced Ca^{2+} release (Torrente et al., 2016). There has been considerable debate on the relative importance of this Ca^{2+} clock mechanism in SAN automaticity with some studies ascribing it a dominant or even essential role and others concluding that the Ca^{2+} clock is an important contributor, but that spontaneous activity in the SAN can continue without it, albeit with reduced rates and/or stability (Lakatta and DiFrancesco, 2009; Honjo et al., 2003; Lakatta et al., 2010). Nevertheless, the evidence is overwhelming that SR Ca^{2+} release occurs during the late DD and this leads to the activation of I_{NCX}, which increases the rate of depolarization during diastole and thus enhances spontaneous AP firing in the SAN.

Further evidence of a role for SR Ca^{2+} release in automaticity comes from studies of IP_3 receptors (IP_3Rs) in the SAN. All three IP_3R subtypes (IP_3R1, IP_3R2, and IP_3R3) are expressed in the heart and IP_3R1 and IP_3R2 have both been detected in the SAN (Ju et al., 2011, 2012). Activation of IP_3Rs with either membrane-permeable IP_3 or indirectly via application of endothelin-1 (which

increases endogenous IP_3 levels via the phospholipase C signaling pathway) caused a significant increase in Ca^{2+} spark frequency near the cell membrane, indicating SR Ca^{2+} release. Furthermore, these IP_3R agonists also increased spontaneous AP generation in the SAN (Ju et al., 2011). Consistent with these findings, IP_3R2 knockout mice as well as pharmacological inhibition of IP_3Rs result in a reduction in spontaneous Ca^{2+} spark frequency and SAN AP firing rate (Ju et al., 2011; Kapoor et al., 2015). Combined, these data indicate IP_3R2-mediated SR Ca^{2+} release can contribute to pacemaker activity in the SAN.

Sustained inward current

The sustained inward current, I_{st}, is a current carried by Na^+ that activates at ~−70 mV and peaks at ~−50 mV. I_{st} is enhanced by β-AR agonists, is insensitive to TTX, and is blocked by dihydropyridine receptor antagonists as well as divalent cations (Mg^{2+}, Ni^{2+}) (Mitsuiye et al., 2000; Cho et al., 2003; Shinagawa et al., 2000; Toyoda et al., 2005). I_{st} has been detected in SAN myocytes and, interestingly, appears to be present only in spontaneously beating, but not quiescent, SAN cells (Mitsuiye et al., 2000; Zhang et al., 2002). Based on its biophysical and kinetic properties, I_{st} has been predicted to contribute to the generation of the DD, particularly in the central regions of the SAN were I_{Na} is small or absent (Shinagawa et al., 2000). The molecular identity of the channels responsible for I_{st} has not yet been identified and until this is accomplished it will remain difficult to determine the precise role of I_{st} in the SAN.

Sodium channels

The heart expresses multiple sodium channel isoforms that can be categorized based on their sensitivity to tetrodotoxin (TTX). The dominant cardiac sodium current (I_{Na}) is carried by the TTX-resistant $Na_V1.5$ channels. $Na_V1.5$ is absent from the center of the SAN (Lei et al., 2004, 2005, 2007), which is consistent with the low V_{max} characteristic of central SAN myocytes. In contrast, $Na_V1.5$, and the resulting I_{Na}, is detected in the larger cells of the peripheral SAN.

TTX-sensitive sodium channels (sometimes referred to as neuronal sodium channels) are also expressed in the heart, including in the SAN. Specifically, $Na_V1.1$ and $Na_V1.3$ subunits have been detected in the mouse SAN (Maier et al., 2003) and $Na_V1.1$, $Na_V1.3$, and $Na_V1.6$ have been identified in the rat SAN (Huang et al., 2015). There is now evidence to suggest that TTX-sensitive Na^+ channels play an important role in pacemaker activity in the SAN. For example, in Langendorff perfused mouse or rat hearts, low concentrations of TTX result in a significant reduction in heart rate (Maier et al., 2003; Huang et al., 2015). Furthermore, in the isolated rabbit SAN, application of nanomolar concentrations of TTX results in a reduction in spontaneous AP firing frequency (Lei et al., 2004).

Detailed investigations have identified differential roles for TTX-sensitive and resistant sodium channels in cardiac pacemaking. In optical mapping studies, nanomolar concentrations of TTX (which would only affect neuronal Na^+ channels) elicit an increase in SAN cycle length, which is consistent with a slower heart rate, but no change in SAN conduction velocity. In contrast, application of micromolar concentrations of TTX (which would block $Na_V1.5$ as well as neuronal Na^+ channels) resulted in a greater increase in cycle length as well as a reduction in conduction velocity across the SAN (Maier et al., 2003). Consistent with these observations, $Na_V1.5$-deficient mice have impaired SAN function resulting in a reduced heart rate attributed to slowed SAN conduction at the peripheral regions of the SAN (Lei et al., 2005). Central SAN myocytes from $Na_V1.5$ knockout mice showed no changes in AP morphology or automaticity while larger peripheral SAN myocytes from $Na_V1.5$ knockout mice had reduced spontaneous AP firing and smaller AP peaks. Collectively, based on these findings, it has been suggested that TTX-sensitive I_{Na} contributes to pacemaker function whereas, TTX-resistant I_{Na} does not contribute to automaticity in the central SAN, but can affect heart rate by modulating conduction through the peripheral SAN and into the atrium (Lei et al., 2004, 2007).

Inward rectifier potassium channels

The inward rectifier K^+ current (I_{K1}) is carried by K^+ channels made up of $K_{ir}2.1$ and K_{ir} 2.2 subunits. I_{K1} is importantly involved in maintaining the resting membrane potential in working contractile myocytes; however, it is largely absent in SAN myocytes. The lack of I_{K1} partly explains the more depolarized MDP in SAN myocytes relative to the hyperpolarized resting membrane potential in contractile myocytes of the surrounding atrium (Mangoni and Nargeot, 2008). It should be noted that while not present in central SAN myocytes, I_{K1} can be measured in peripheral SAN myocytes although at much lower densities than in the working myocardium (Cho et al., 2003; Mangoni and Nargeot, 2001).

Delayed rectifier potassium channels

The ether-a-go-go family of proteins are responsible for the rapidly activating delayed rectifier potassium current (I_{Kr}), which is blocked by compounds such as E-4031 and dofetilide. The slow delayed rectifier K^+ current (I_{Ks}) is encoded by KCNQ1 in the heart and is sensitive to chromonol 293B. Both of these delayed rectifier currents have been described in the SAN, with some species differences as noted later.

In mouse SAN myocytes, three splice variants for mERG1 (1a, 1a′, and 1b) are expressed (Clark et al., 2004). E-4031 application results in depolarization of the MDP, a reduced AP amplitude and can completely prevent spontaneous AP firing in SAN myocytes (Ono and Ito, 1995; Verheijck et al., 1995). Experiments performed in rabbit heart indicate that a gradient of I_{Kr} is present across the SAN such that the effect of E-4031 is greater in the center of the SAN compared with the periphery (Kodama et al., 1999).

Functionally, I_{Kr} contributes to repolarization of the AP and determines the MDP in SAN myocytes (Clark et al., 2004; Verheijck et al., 1995). Furthermore, kinetic analysis of I_{Kr} indicates that these channels have an accelerated rate of deactivation, but I_{Kr} may not deactivate fully during the cardiac cycle so that a sustained current may be present throughout the DD. Inhibition of I_{Kr} shifts

the MDP and prolongs AP repolarization resulting in a slowing of spontaneous AP firing. This slowing effect is largely due to less activation of I_f and Ca^{2+} channels.

While I_{Kr} appears to the dominant delayed rectifier K^+ current in rabbit and rodent SAN, in the pig SAN I_{Ks} has been found to be responsible for repolarization of the SAN AP (Ono et al., 2000). In the pig, I_{Ks} appears to function in the same way as I_{Kr}. Consistent with this, block of I_{Ks} in pig SAN with chromanol 293B halts spontaneous AP firing in a similar fashion to E-4031 in rabbit SAN.

Transient outward potassium channels

The transient outward potassium current (I_{to}) plays a critical role in the working myocardium, but is less well understood in the SAN. I_{to} is characterized by fast activation and inactivation kinetics and can be subdivided into fast and slow components based on differences in inactivation kinetics. The fast component of I_{to} ($I_{to,f}$) is encoded by $K_V4.2$ and $K_V4.3$, whereas the slow component ($I_{to,s}$) is encoded by $K_V1.4$ (Nerbonne and Kass, 2005).

I_{to} density is significantly lower in rabbit SAN myocytes as compared to atrial myocytes (Uese et al., 1999). Within the SAN, sensitivity to the I_{to} channel blocker 4-aminopyradine (4-AP) was correlated with cell size such that larger SAN myocytes (presumably from the peripheral SAN) exhibited larger responses to 4-AP compared with the smaller cells from the center of the SAN (Lei et al., 2000). Consistent with these observations, 4-AP also results in AP prolongation in isolated SAN, but the effect is more pronounced in larger SAN myocytes. Collectively, these findings demonstrate that I_{to} is functional in the SAN, perhaps more prominently in the SAN periphery, but more studies are needed to determine the precise role of I_{to} in regulating SAN function.

Two-pore potassium channels

Two-pore domain potassium channels (K_{2P}) are a family of K^+ channels with emerging roles in the heart. Functionally, they facilitate stabilization of the resting membrane potential and AP repolarization in cardiomyocytes (Wiedmann et al., 2016). K_{2P} channels are not voltage dependent; rather they continually conduct currents throughout the various phases of the AP and are hence referred to as background K^+ currents. Regulation of these channels is diverse, and includes factors such as temperature, pH, lipids, and membrane stretch. Six subfamilies of K_{2P} channels exist with the TWIK (two-pore domain weak rectifying potassium channel), TREK (TWIK-related potassium channel), and TASK (TWIK-related acid-sensitive potassium channel) subfamilies being expressed in the heart (Wiedmann et al., 2016; Gaborit et al., 2007).

Emerging evidence is suggestive of a role for K_{2P} channels in SAN electrophysiology. For example, the stretch-sensitive TREK channel is expressed in the mouse SAN and TREK-1 knockout mice have a reduced heart rate (Unudurthi et al., 2016). SAN myocytes isolated from TREK-1-deficient animals exhibit an increased rate of DD and spontaneous AP firing rate as well as an increase in APD at 50% repolarization. Furthermore, background K^+ current was significantly reduced in isolated SAN myocytes from TREK-1 knockout mice. Thus, TREK-1 contributes to SAN automaticity by altering the rate of DD. Additional studies are needed to further investigate the role of K_{2P} channels in the SAN.

Calcium-activated potassium channels

Three types of calcium-activated K^+ channels have been categorized based on their single-channel conductance, including the big conductance (BK), intermediate conductance (IK), and small conductance (SK) channels. These channels are coupled to L-type Ca^{2+} channels and, as their name suggests, are activated by an increase in intracellular calcium levels (Schmitt et al., 2014). Relatively little is known about the role of these channels in the SAN, however emerging evidence is suggestive of a role for BK channels in SAN excitability. Both pharmacological inhibition and genetic ablation of BK channels in isolated SAN myocytes leads to a significant reduction in spontaneous AP firing with a corresponding increase in DD duration (Lai et al., 2014). A role for SK channels has also been proposed in the SAN (Weisbrod et al., 2016).

TRP channels

TRP channels are a large and diverse family of ion channels divided into a number of subfamilies, including the short canonical (TRPC) channels, the vanilloid receptor (TRPV) channels, the melastatin (TRPM) channels, the Ankyrin-repeat (TRPA) channels, the polycystin (TRPP) channels, and the mucolipin (TRPML) channels (Clapham et al., 2001, 2003). Within each of these subfamilies a number of channel isoforms exist. Several TRP channels have been implicated in SAN function including TRPM7, TRMP4, and TRPC channels.

TRPM7 channels are permeable to divalent cations and generate an outwardly rectifying current. Furthermore, TRPM7 is expressed in the SAN and TRPM7 currents are readily detectable in isolated SAN myocytes (Sah et al., 2013). Targeted global knockout of TRPM7 as well as inducible SAN restricted deletion of TRPM7 in mice results in the generation of sinus pauses and AVN block (Sah et al., 2013). Consistent with these observations, TRPM7 knockout mice display a reduction in spontaneous AP frequency in association with a reduction in the DD slope in SAN myocytes. Interestingly the effects of TRPM7 ablation on DD slope appear not to be related directly to the loss of TRPM7 current. Rather, TRPM7 knockout mice display a substantial reduction in HCN channel expression and I_f current density, which appears to account for the reduction in DD slope. Consistent with this hypothesis, a TRPM7 blocker, FTY720, did not affect spontaneous AP frequency in the SAN (Sah et al., 2013).

TRPM4 is a calcium-activated nonselective cation channel that is permeable to Na^+ and K^+, but not Ca^{2+} ions (Little and Mohler, 2013). TRMP4 is activated by intracellular calcium and phosphatidylinositol 4,5-bisphosphate, but inhibited by increases in intracellular ATP. TRPM4 is expressed in the mouse SAN and a nonselective cation current with the properties of TRPM4 currents has been measured in mouse SAN myocytes (Demion et al., 2007). Furthermore, pharmacological inhibition of TRPM4 with

9-phenanthrol or genetic deletion of TRMP4 results in a significant reduction in beating rate within the right atria (Hof et al., 2013). These effects have been attributed to a decrease in the rate of DD as assessed by microelectrode recordings in multicellular atrial preparations. Interestingly, this effect was greater at lower beating rates, thereby suggesting TRPM4 functions in preventing bradycardia. Importantly, the effects of TRPM4 deletion have yet to be studied in isolated SAN myocytes.

The mouse SAN has also been shown to express a number of TRPC channel transcripts, including TRPC1, 2, 3, 4, 6, and 7 and it has been suggested that one or more of these TRPC channels may be involved in mediating Ca^{2+} influx into SAN myocytes in a store operated fashion (Ju et al., 2007). Consistent with this hypothesis, Gd^{3+} and SKF-96355, two compounds known to antagonize several TRPC channels, were shown to block Ca^{2+} entry into SAN myocytes. Furthermore, SKF-96365 reduced pacemaker activity (Ju et al., 2007). While these findings are very interesting, it must be noted that many of the pharmacological agents used in these studies are not specific to TRPC channels and more work is needed to determine the precise role of TRPC channels in the SAN.

AVN Ion Channels

Like SAN myocytes, myocytes isolated from the AVN are characterized by their ability to generate spontaneous APs with DDs. Spontaneous AP frequency in AVN myocytes is lower than in SAN myocytes and less is known about ion channel function in the AVN. At the molecular level, mRNA transcripts for HCN1, HCN4, $Na_V1.1$, $Ca_V1.3$, $Ca_V3.1$, $K_{ir}3.4$, and Cx45 have been detected in the AVN and these transcripts are expressed at higher levels compared with the surrounding atrial myocardium (Greener et al., 2011; Marionneau et al., 2005). On the other hand, $Na_V1.5$, $K_{ir}2.1$, and Cx43 expression was lower in the AVN compared with the atrium.

Consistent with their ability to intrinsically generate spontaneous APs, AVN cells display a prominent I_f, although I_f density in the AVN is ~50% smaller than in the SAN (Marger et al., 2011a,b; Mesirca et al., 2014). While I_f is detected throughout the AVN, regional differences exist such that I_f in nodal or nodo-his cells is significantly higher compared with atrio-nodal cells (Munk et al., 1996; Choisy et al., 2015).

Similar to the SAN, sodium channel expression is variable within the AVN. The compact AVN lacks I_{Na}, which is consistent with the low V_{max} characteristic of the AVN (Efimov et al., 2004; Greener et al., 2011). On the other hand, I_{Na} is detected in all atrio-nodal cells and approximately one-third of nodo-his cells in rabbit and Guinea-pig hearts (Munk et al., 1996; Yuill and Hancox, 2002). Furthermore, both TTX-resistant and TTX-sensitive I_{Na} have been recorded from isolated rabbit AVN myocytes, and blockade of these channels using high levels of TTX can result in cessation of spontaneous AP firing (Marger et al., 2011b).

Multiple K^+ currents have been identified in AVN myocytes. I_{to} density is variable within the AVN such that it is more commonly detected in atrio-nodal cells compared with nodal cells (Marger et al., 2011b; Munk et al., 1996). In mouse AVN, the delayed rectifier I_{Kr} has been identified and found to be larger than in SAN myocytes (Marger et al., 2011b; Efimov et al., 2004). I_{Ks}, on the other hand, was not detected in mouse AVN myocytes. I_{K1} has been recorded in AVN myocytes from mouse and rabbit AVN myocytes (Choisy et al., 2015).

In AVN myocytes, both $I_{Ca,T}$ and $I_{Ca,L}$ contribute to automaticity and AVN function and transcripts for several Ca^{2+} channels can be detected including $Ca_V1.2$, $Ca_V1.3$, and $Ca_V3.1$ (Marger et al., 2011a,b; Marionneau et al., 2005). $I_{Ca,L}$ in the AVN is approximately half the magnitude of that in the SAN and application of L-type Ca^{2+} channel blockers can completely suppress spontaneous APs (Marger et al., 2011a; Greener et al., 2011). $I_{Ca,L}$ density is approximately twice as large in rabbit AVN as compared with mouse AVN (Choisy et al., 2015).

Consistent with an important role for Ca^{2+} channels in AVN function, $Ca_V3.1$ knockout mice are characterized by prolongation of the P–R and P–Q intervals (indicators of conduction through the AVN) and a significant increase in AVN effective refractory period (Mangoni et al., 2006b; Marger et al., 2011a). Furthermore, $Ca_V1.3$ knockout mice show a greater prolongation of the PR interval than $Ca_V3.1$ knockout mice. This prolongation of the P-R interval is exacerbated in double knockouts lacking both Cav1.3 and Cav3.1. In isolated AVN myocytes, the generation of spontaneous APs was reduced by 70% in $Ca_V3.1$ knockout mice and absent in Cav1.3 knockout animals.

SK2 knockout mice exhibit impaired SAN and AVN function, as indicated by a reduction in heart rate and prolongation of the P–R interval (Zhang et al., 2008). AP firing frequency, the rate of DD, and V_{max} were reduced, whereas APDs were prolonged in the AVN of SK2 knockout mice. In contrast, overexpression of SK2 results in the opposite effects, including an increase in spontaneous AP firing rate (Zhang et al., 2008). These effects were attributed to alterations in I_{KCa} densities in AVN myocytes. Combined, these data indicate SK2 channels contribute to AVN function.

SR calcium release also affects AVN function. In isolated rabbit AVN cells, calcium transients correlate with AP generation (Hancox et al., 1994). These Ca^{2+} transients result in an increase in intracellular calcium at the periphery of the myocyte that subsequently spreads throughout the cell. Pharmacological inhibition of SERCA pumps leads to a significant reduction in Ca^{2+} transients and slowed the frequency of AP generation. Furthermore, interfering with SR calcium release by application of ryanodine significantly decreases Ca^{2+} transient amplitude in the AVN. This in turn slows the rate of spontaneous APs in AVN myocytes (Ridley et al., 2008; Choisy et al., 2015). There is also data to suggest SR Ca^{2+} release is coupled to I_{NCX} because inhibition of NCX prevents spontaneous Ca^{2+} transients in AVN (Ridley et al., 2008). Combined, these data indicate both SR calcium release and I_{NCX} facilitate the generation of spontaneous APs in the AVN, although compared to the SAN this is relatively poorly understood.

Regulation by the Autonomic Nervous System

The SAN and AVN are both heavily innervated, allowing heart rate and conduction through the AVN to be altered by the release of neurotransmitters (Pauza et al., 2013, 2014). The autonomic nervous system can be divided into two branches including the sympathetic nervous system (SNS) and parasympathetic nervous system (PNS). Stimulation of the β-ARs by SNS agonists results in an increase in heart rate, whereas stimulation of muscarinic (M_2) receptors by the PNS results in a decrease in heart rate. The interplay between sympathovagal activity, combined with the intrinsic activity of the SAN, determines the rate of spontaneous AP firing in SAN myocytes and hence the heart rate (Mangoni and Nargeot, 2008).

β-AR activation by catecholamines results in the activation of stimulatory G proteins (G_s) that cause an increase in cAMP production by adenylyl cyclases and an increase in protein kinase A (PKA) activity. Increasing cAMP levels and PKA activity causes a positive chronotropic effect and enhances conduction through the AVN following the activation of a number of targets including ion channels and SR Ca^{2+} handling.

In isolated SAN myocytes, β-AR activation leads to a rapid increase in the slope of the DD and a subsequent increase in spontaneous AP firing frequency without affecting APD (Accili et al., 2002; Irisawa et al., 1993) (**Fig. 4**). I_f is modulated by cAMP following the direct binding of cAMP to HCN channels (DiFrancesco and Tortora, 1991), which causes a positive shift in the I_f activation curve and increases I_f during the DD. These effects of cAMP on I_f have been largely thought to occur independently of PKA, although recent evidence suggests that HCN channels can also be phosphorylated by PKA (Liao et al., 2010).

L-type Ca^{2+} currents contribute to the increase in spontaneous AP firing in the SAN following β-AR activation. Consistent with this hypothesis, ISO can dose-dependently increase $I_{Ca,L}$ in SAN myocytes with similar efficacy to I_f (Zaza et al., 1996). Furthermore, SAN myocytes isolated from $Ca_V1.3$ knockout mice show a blunted response to ISO, including impaired effects on DD slope and AP firing frequency (Torrente et al., 2016). β-AR agonists are thought to modulate $I_{Ca,L}$ ($Ca_V1.2$ and $Ca_V1.3$) in a PKA-dependent fashion (Mangoni and Nargeot, 2008).

SR Ca^{2+} release is also modulated by β-AR agonists and it has been suggested that this makes a major contribution to the effects of the SNS on AP firing in the SAN (Lakatta et al., 2010). Enhancement of intracellular cAMP, PKA, and CaMKII activity following β-AR activation leads to an increase in SR Ca^{2+} spark amplitude, frequency, and SR filling rate (Vinogradova et al., 2006; Gao et al., 2011). These effects have been attributed to increases in phosphorylation of ryanodine receptors and phospholamban. In SAN and AVN myocytes, these effects result in increased SR calcium release, which enhances I_{NCX} during the DD and increases AP firing frequency (Vinogradova et al., 2002; Gao et al., 2011; Hancox et al., 1994). The relative importance of each of these mechanisms (I_f, $I_{Ca,L}$ SR Ca^{2+} release) in mediating the positive chronotropic effects of SNS activation has not been resolved.

PNS (i.e., vagus nerve) stimulation causes a negative chronotropic effect and slowing of conduction in the SAN and AVN following the release of acetylcholine (ACh), which activates M_2 receptors and inhibitory G proteins ($G_{i/o}$) (Irisawa et al., 1993). The α_i subunit of these G proteins inhibits AC activity and cAMP signaling. Reduced cAMP levels decrease the DD slope in SAN myocytes and these effects can involve reductions in I_f, $I_{Ca,L}$, and SR Ca^{2+} release (Mangoni and Nargeot, 2008; Lakatta et al., 2010) (**Fig. 4**). In addition to these effects, the βγ subunits of the $G_{i/o}$ proteins can directly activate GIRK ($K_{ir3.x}$) channels that mediate I_{KACh} currents (Mangoni and Nargeot, 2008). Activation of I_{KACh} hyperpolarizes the SAN myocyte, which also slows spontaneous AP firing. A significant amount of investigation has gone into trying to determine which ionic mechanism(s) are particularly important for the negative chronotropic effects of PNS agonists. For example, $K_{ir3.4}$ or $G_{\beta\gamma}$ knockout mice have significant reductions in PNS responsiveness, indicating that I_{KACh} makes a major contribution to the response (Wickman et al., 1998; Gehrmann et al., 2002; Mesirca et al., 2016a). On the other hand, biophysical studies have suggested that I_f is more sensitive to acetylcholine than I_{KACh} or $I_{Ca,L}$ (DiFrancesco et al., 1989; Zaza et al., 1996). From these studies it was concluded that I_f contributes more importantly to changing pacemaker activity in the SAN. Still other studies have shown that PNS agonists suppress local Ca^{2+} releases from the SR during the DD and this is a major determinant of the slowing in pacemaker activity, including in conditions where I_{KACh} would not be activated (Lyashkov et al., 2009; van Borren et al., 2010). Additional studies will be required to resolve these issues.

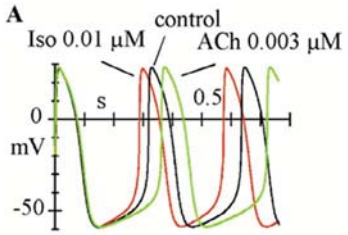

Fig. 4 Effects of the β-adrenergic receptor agonist ISO and the muscarinic agonist acetylcholine (ACh) on spontaneous action potential cycle length and diastolic depolarization slope in the sinoatrial node. Note that these autonomic nervous system agonists modulate action potential cycle length in association with changes in the slope of the diastolic depolarization. Reproduced with permission from Accili, E.A., Proenza, C., Baruscotti, M. and Difrancesco, D. (2002). From funny current to HCN channels: 20 years of excitation. News in Physiological Sciences 17, 32–37.

Hormonal Regulation of the SAN by Natriuretic Peptides

Natriuretic peptides (NPs) are a family of hormones with a number of potent effects in the cardiovascular system (Potter et al., 2006; Kuhn, 2004). Several members of the NP family have been identified including atrial NP (ANP), B-type NP (BNP), and C-type NP (CNP). Each of these peptides is expressed in the heart and is present in both cardiomyocytes and cardiac fibroblasts (Moghtadaei et al., 2016b).

Three NP receptors, called NPR-A, NPR-B, and NPR-C, mediate the effects of NPs (Potter et al., 2006). NPR-A (which binds ANP and BNP) and NPR-C (which is selectively activated by CNP) are guanylyl cyclase (GC) linked receptors that enhance cGMP signaling (Lucas et al., 2000) while NPR-C (which binds all NPs with similar affinity) is coupled to inhibitory G proteins that inhibit AC signaling (Rose and Giles, 2008; Anand-Srivastava, 2005).

NPs can potently regulate heart rate through effects on pacemaker myocytes in the SAN (Springer et al., 2012; Azer et al., 2012; Rose et al., 2007). In isolated SAN myocytes, BNP and CNP each increase spontaneous AP firing frequency in association with increases in the DD slope and APD, but without differences in MDP. These effects on SAN AP firing occurred in association with increases in HR in intact hearts. Voltage clamp studies demonstrate that these changes in AP firing properties were the result of increases in I_f and total $I_{Ca,L}$ in the presence of BNP or CNP along with shifts in the voltage dependence of channel activation ($V_{1/2\,(act)}$). To determine the mechanism for these electrophysiological effects, NPR-C knockout (NPR-C$^{-/-}$) mice and pharmacological approaches have been used. The stimulatory effects of BNP and CNP on spontaneous AP firing, I_f and $I_{Ca,L}$ in NPR-C$^{-/-}$ mice are indistinguishable from wild-type mice in basal conditions. In contrast, the effects of BNP and CNP were occluded by the PDE3 inhibitor milrinone and the effects of BNP were antagonized following NPR-A blockade. Thus, these experiments illustrate that BNP and CNP can potently increase HR and spontaneous AP firing in SAN myocytes by activating the GC-linked NPR-A and NPR-B receptors and inhibiting PDE3 activity (Springer et al., 2012). Consistent with these findings, ANP has also been shown to elicit a cGMP-dependent increase in I_f in human atrial myocytes (Lonardo et al., 2004).

Although NPR-C does not affect SAN function in basal conditions, it does contribute importantly in the presence of β-adrenergic receptor (β-AR) activation (Azer et al., 2012; Springer et al., 2012). Specifically, in the presence of ISO, cANF dose-dependently decreases HR and slows spontaneous AP firing by decreasing the DD slope in SAN myocytes (Azer et al., 2012). These effects of cANF are completely absent in NPR-C$^{-/-}$ mice confirming they are mediated by the NPR-C receptor. To explore the contributions of different NPRs to these responses, we compared the effects of BNP and CNP (which can activate NPR-A/B as well as NPR-C) to cANF (which only activates NPR-C). These measurements show that BNP and CNP increase HR and AP firing in submaximal (10 nM) doses of ISO, but these effects are smaller than those observed in basal conditions because, in the presence of ISO, BNP, and CNP activate NPR-A/B (which mediate an increase in HR and AP firing) as well as NPR-C (which mediates a decrease in HR and AP firing). Interestingly, in the presence of maximum doses of ISO (1 μM) BNP and CNP elicit reductions in HR and cause slowing of spontaneous AP firing in SAN myocytes due to a greater contribution from NPR-C. In agreement with this observation, CNP and cANF can also decrease $I_{Ca,L}$ in SAN myocytes in the presence of maximum doses of ISO (Rose et al., 2004). These changes in ion channel function and AP firing properties correlate with changes in SAN activation and conduction patterns that are also differentially modulated by the GC-linked NPRs and NPR-C (Azer et al., 2014). Collectively, these studies demonstrate that NPs can modulate SAN function via the NPR-A/B receptors (stimulatory) and NPR-C (inhibitory) and that these receptors elicit opposing effects. Because of this, NPs can increase HR and SAN function in some conditions, but decrease HR in others and this is dependent on the extent of β-AR activation and the relative contribution of each NPR in different physiological conditions (Azer et al., 2012, 2014; Moghtadaei et al., 2016b). In addition to these effects of NPs on SAN myocyte function, NPs also regulate collagen deposition, and hence electrical conduction, in the SAN. Consistent with this, genetic loss of NPR-C results in SAN dysfunction in association with enhanced fibrosis and slowed conduction in the SAN (Egom et al., 2015).

Mechanical Effects on the SAN

Mechanical effects on SAN activity (Quinn and Kohl, 2012) were first recognized in 1915 by Francis Bainbridge, who found that intravenous fluid injections in anesthetized dogs resulted in right atrial distension and increased beating rate (Bainbridge, 1915) (similar effects have been observed since in a wide variety of vertebrates (Pathak, 1973), including human (Donald and Shepherd, 1978)). Stretch-induced increases in beating rate also occur in the isolated (decentralized) heart (Blinks, 1956), SAN tissue (Blinks, 1956; Deck, 1964), and SAN cells (Craelius et al., 1988; Iribe et al., 2007), and are insensitive to ablation of intracardiac neurons (Wilson and Bolter, 2002), block of neuronal Na^+ channels (Chiba, 1977; Wilson and Bolter, 2002), and adrenergic and cholinergic blockade (Blinks, 1956; Brooks et al., 1966; Chiba, 1977; Wilson and Bolter, 2002), indicating that nonneuronal, intracardiac mechanisms must be involved.

Microelectrode recordings in cat and rabbit right atrial tissue have demonstrated that stretch increases SAN MDP, reduces maximum systolic membrane potential, and increases DD rate (Deck, 1964). Patch-clamp recordings in axially stretched isolated rabbit SAN cells, combined with computational modeling, have established that this can be explained by a mechanosensitive whole-cell current with a reversal potential of ∼10 mV (Cooper et al., 2000). This current is presumably carried by cation nonselective stretch-activated channels, which are rapidly activating, with a reversal potential between 0 and −20 mV in cardiac cells (Craelius et al., 1988; Guharay and Sachs, 1984), and whose block causes a reversible reduction of stretch-induced changes in beating rate (Cooper and Kohl, 2005). In fact, even if located outside of SAN cells in electrically coupled nonmyocytes (Quinn et al., 2016), cation nonselective stretch-activated channels can account for stretch effects, as they are found in fibroblasts

(Stockbridge and French, 1988), which are coupled to SAN cells in rabbit (Camelliti et al., 2004), and are depolarized by stretch (Kohl and Noble, 1996; Kohl et al., 1994).

Stretch may also affect fundamental components of SAN function. When expressed in oocytes, current amplitude (Calloe et al., 2005) and activation and deactivation rate (Lin et al., 2007) of HCN channels are increased with mechanical stimulation. Similarly, Ca^{2+} ($Ca_V1.2$) (Calabrese et al., 2002; Lyford et al., 2002) Na^+ ($Na_V1.5$ and $Na_V1.6$), and K^+ (Kv1, Kv3, Kv7, and KvCa) (Morris, 2011) channels are mechanically modulated in various expression systems. Axial stretch of guinea-pig (Iribe and Kohl, 2008) or rat (Gamble et al., 1992; Prosser et al., 2011, 2013; Iribe et al., 2009) ventricular myocytes, on the other hand, causes an acute increase in Ca^{2+} sparks (spontaneous Ca^{2+} release from the SR). This effect apparently occurs via augmented ryanodine receptor open probability (Iribe et al., 2009), which may involve local activation by mechanically induced mitochondrial Ca^{2+} release through the mitochondrial NCX (Belmonte and Morad, 2008), a channel whose current alters beating rate in isolated rabbit SAN cells by affecting Ca^{2+} spark frequency (Yaniv et al., 2012). Thus, if any of these effects occurs also in SAN cells, they may contribute to stretch-induced changes in beating rate.

In the whole heart, stretch of SAN tissue will vary regionally and with time. The SAN is structurally heterogeneous, resulting in regional differences in stiffness. Changes in beating rate during externally applied force correlate best with maximum tissue deformation, which occurs at the periphery of the SAN, a region more distensible than the central node (Kamiyama et al., 1984). This difference could be important for transmission of electrical activity from the SAN to atrium (Garny et al., 2003), as the SAN periphery is where (the possibly mechanosensitive) HCN channels are thought to play the largest role in SAN activity (due to the more negative diastolic potential in that region) (Kreitner, 1985; Nikmaram et al., 1997). At the same time, SAN stretch will be greatest at the end of atrial filling, which is when SAN cells are moving toward AP initiation. In this way, mechanical priming of SAN cells could adjust function on a beat-by-beat basis to diastolic load, contributing to the matching of cardiac output (beating rate × stroke volume) to venous return (and may also play a role in respiratory sinus arrhythmia, as it continues to exist in the decentralized, transplanted heart (Bernardi et al., 1989)). Moreover, it appears that physiological loading may be essential to SAN automaticity, as slack tissue often shows no or irregular rhythm, while moderate stretch can restore normal activity (Brooks et al., 1966) (although excessive stretch can induce arrhythmias (Brooks et al., 1966; Hoffman and Cranefield, 1960), so pathophysiological loading during atrial overload may unbalance pacemaker mechanisms). This apparent requirement for a minimum mechanical stimulus is also apparent during ontogenetic initiation of the first heartbeat, as fluid pressure build-up in the quiescent cardiac tube appears to be required for the initiation of its spontaneous activity (Rajala et al., 1977).

There is also evidence supporting an interaction between mechanical and autonomic beating rate modulation. In intact rabbit (Bolter and Wilson, 1999; Bolter, 1994), and isolated atria of rabbit (Bolter, 1996), guinea-pig (Wilson and Bolter, 2001), and rat (Barrett et al., 1998), an increase in right atrial pressure induces both beating rate acceleration and a significant reduction in the percentage response to vagal stimulation. Vice versa, when beating rate is reduced by vagal stimulation the stretch-induced beating rate response is augmented, an interaction that may be mediated by I_{KACh}, as it is reduced with increased right atrial pressure (Han et al., 2010). In this way, parasympathetic control of beating rate may be continuously modified by atrial loading, further contributing to the stretch-induced adjustment of BR to fluctuations in venous return, and helping prevent excessive slowing and diastolic distension, while maintaining cardiac output and adequate circulation (Brooks and Lange, 1977).

Conclusions

Since the discovery of the SAN in 1907 and the AVN in 1906 substantial progress has been made in our understanding of the cellular and molecular mechanisms for spontaneous activity in these specialized pacemaker regions of the heart. These discoveries have been instrumental in facilitating a comprehensive understanding of cardiac electrical conduction. While progress has been considerable, there is still much to be learned, as noted throughout the preceding text. Continuing to unravel the precise determinants of cellular function in the SAN and AVN, and how each is regulated, is of paramount importance because dysfunction in each of these regions can contribute in important ways to cardiovascular disease.

Current treatments for SAN and AVN disease often involve implantation of artificial pacemakers which, while effective, come with a number of attendant risks and limitations. Because of this, and in parallel with the continued generation of novel insight into the mechanisms for automaticity, the field of biological pacing, which seeks to engineer zones of focal spontaneous electrical activity in regions of myocardium that are normally quiescent, has blossomed (Cho, 2015; Rosen et al., 2011). Such approaches, if successful, would free the patient from all hardware associated with traditional artificial pacemakers. Given the challenges associated with correcting SAN and/or AVN disease, motivation should remain high to continue to improve our understanding of the basis for automaticity in the heart with the hopes that this knowledge will inform the next generation of therapeutics targetting these specialized regions of the heart.

References

Accili EA, Proenza C, Baruscotti M, and Difrancesco D (2002) From funny current to HCN channels: 20 years of excitation. *News in Physiological Sciences* 17: 32–37.

Anand-Srivastava MB (2005) Natriuretic peptide receptor-C signaling and regulation. *Peptides* 26: 1044–1059.

Anderson RH and Ho SY (1998) The architecture of the sinus node, the atrioventricular conduction axis, and the internodal atrial myocardium. *Journal of Cardiovascular Electrophysiology* 9: 1233–1248.

Anderson RH, Janse MJ, van Capelle FJ, Billette J, Becker AE, and Durrer D (1974) A combined morphological and electrophysiological study of the atrioventricular node of the rabbit heart. *Circulation Research* 35: 909–922.

Anderson RH and Latham RA (1971) The cellular architecture of the human atrioventricular node, with a note on its morphology in the presence of a left superior vena cava. *Journal of Anatomy* 109: 443–455.

Anderson RH, Yanni J, Boyett MR, Chandler NJ, and Dobrzynski H (2009) The anatomy of the cardiac conduction system. *Clinical Anatomy* 22: 99–113.

Azer J, Hua R, Krishnaswamy PS, and Rose RA (2014) Effects of natriuretic peptides on electrical conduction in the sinoatrial node and atrial myocardium of the heart. *The Journal of Physiology* 592: 1025–1045.

Azer J, Hua R, Vella K, and Rose RA (2012) Natriuretic peptides regulate heart rate and sinoatrial node function by activating multiple natriuretic peptide receptors. *Journal of Molecular and Cellular Cardiology* 53: 715–724.

Bainbridge FA (1915) The influence of venous filling upon the rate of the heart. *The Journal of Physiology* 50: 65–84.

Barrett CJ, Bolter CP, and Wilson SJ (1998) The intrinsic rate response of the isolated right atrium of the rat, Rattus norvegicus. *Comparative Biochemistry and Physiology. Part A, Molecular & Integrative Physiology* 120: 391–397.

Bartos DC, Grandi E, and Ripplinger CM (2015) Ion channels in the heart. *Comprehensive Physiology* 5: 1423–1464.

Baruscotti M, Barbuti A, and Bucchi A (2010) The cardiac pacemaker current. *Journal of Molecular and Cellular Cardiology* 48: 55–64.

Baruscotti M, Bucchi A, Viscomi C, Mandelli G, Consalez G, Gnecchi-Rusconi T, Montano N, Casali KR, Micheloni S, Barbuti A, and Difrancesco D (2011) Deep bradycardia and heart block caused by inducible cardiac-specific knockout of the pacemaker channel gene HCN4. *Proceedings of the National Academy of Sciences of the United States of America* 108: 1705–1710.

Belmonte S and Morad M (2008) 'Pressure-flow'-triggered intracellular Ca^{2+} transients in rat cardiac myocytes: Possible mechanisms and role of mitochondria. *The Journal of Physiology* 586: 1379–1397.

Bernardi L, Keller F, Sanders M, Reddy PS, Griffith B, Meno F, and Pinsky MR (1989) Respiratory sinus arrhythmia in the denervated human heart. *Journal of Applied Physiology* 67: 1447–1455.

Bleeker WK, Mackaay AJ, Masson-Pevet M, Bouman LN, and Becker AE (1980) Functional and morphological organization of the rabbit sinus node. *Circulation Research* 46: 11–22.

Blinks JR (1956) Positive chronotropic effect of increasing right atrial pressure in the isolated mammalian heart. *The American Journal of Physiology* 186: 299–303.

Bolter CP (1994) Intrinsic cardiac rate regulation in the anaesthetized rabbit. *Acta Physiologica Scandinavica* 151: 421–428.

Bolter CP (1996) Effect of changes in transmural pressure on contraction frequency of the isolated right atrium of the rabbit. *Acta Physiologica Scandinavica* 156: 45–50.

Bolter CP and Wilson SJ (1999) Influence of right atrial pressure on the cardiac pacemaker response to vagal stimulation. *The American Journal of Physiology* 276: R1112–R1117.

Boyett MR, Dobrzynski H, Lancaster MK, Jones SA, Honjo H, and Kodama I (2003) Sophisticated architecture is required for the sinoatrial node to perform its normal pacemaker function. *Journal of Cardiovascular Electrophysiology* 14: 104–106.

Boyett MR, Honjo H, and Kodama I (2000) The sinoatrial node, a heterogeneous pacemaker structure. *Cardiovascular Research* 47: 658–687.

Boyett MR, Honjo H, Yamamoto M, Nikmaram MR, Niwa R, and Kodama I (1999) Downward gradient in action potential duration along conduction path in and around the sinoatrial node. *The American Journal of Physiology* 276: H686–H698.

Brooks CM and Lange G (1977) Interaction of myogenic and neurogenic mechanisms that control heart rate. *Proceedings of the National Academy of Sciences of the United States of America* 74: 1761–1762.

Brooks CM, Lu HH, Lange G, Mangi R, Shaw RB, and Geoly K (1966) Effects of localized stretch of the sinoatrial node region of the dog heart. *The American Journal of Physiology* 211: 1197–1202.

Bucchi A, Barbuti A, Difrancesco D, and Baruscotti M (2012) Funny current and cardiac rhythm: Insights from HCN knockout and transgenic mouse models. *Frontiers in Physiology* 3: 240.

Bucchi A, Baruscotti M, Robinson RB, and Difrancesco D (2007) Modulation of rate by autonomic agonists in SAN cells involves changes in diastolic depolarization and the pacemaker current. *Journal of Molecular and Cellular Cardiology* 43: 39–48.

Calabrese B, Tabarean IV, Juranka P, and Morris CE (2002) Mechanosensitivity of N-type calcium channel currents. *Biophysical Journal* 83: 2560–2574.

Calloe K, Elmedyb P, Olesen SP, Jorgensen NK, and Grunnet M (2005) Hypoosmotic cell swelling as a novel mechanism for modulation of cloned HCN2 channels. *Biophysical Journal* 89: 2159–2169.

Camelliti P, Green CR, Legrice I, and Kohl P (2004) Fibroblast network in rabbit sinoatrial node: Structural and functional identification of homogeneous and heterogeneous cell coupling. *Circulation Research* 94: 828–835.

Chandler NJ, Greener ID, Tellez JO, Inada S, Musa H, Molenaar P, Difrancesco D, Baruscotti M, Longhi R, Anderson RH, Billeter R, Sharma V, Sigg DC, BOYETT MR, and Dobrzynski H (2009) Molecular architecture of the human sinus node: Insights into the function of the cardiac pacemaker. *Circulation* 119: 1562–1575.

Chiba S (1977) Pharmacologic analysis of stretch-induced sinus acceleration of the isolated dog atrium. *Japanese Heart Journal* 18: 398–405.

Cho HC (2015) Pacing the heart with genes: Recent progress in biological pacing. *Current Cardiology Reports* 17: 65.

Cho HS, Takano M, and Noma A (2003) The electrophysiological properties of spontaneously beating pacemaker cells isolated from mouse sinoatrial node. *The Journal of Physiology* 550: 169–180.

Choisy SC, Cheng H, Orchard CH, James AF, and Hancox JC (2015) Electrophysiological properties of myocytes isolated from the mouse atrioventricular node: L-type ICa, IKr, If, and Na-Ca exchange. *Physics Reports* 3:e12633.

Christel CJ, Cardona N, Mesirca P, Herrmann S, Hofmann F, Striessnig J, Ludwig A, Mangoni ME, and Lee A (2012) Distinct localization and modulation of Cav1.2 and Cav1.3 L-type Ca2+ channels in mouse sinoatrial node. *The Journal of Physiology* 590: 6327–6342.

Christoffels VM, Smits GJ, Kispert A, and Moorman AF (2010) Development of the pacemaker tissues of the heart. *Circulation Research* 106: 240–254.

Clapham DE, Montell C, Schultz G, Julius D and International Union of Pharmacology (2003) International Union of Pharmacology. XLIII. Compendium of voltage-gated ion channels: Transient receptor potential channels. *Pharmacological Reviews* 55: 591–596.

Clapham DE, Runnels LW, and Strubing C (2001) The TRP ion channel family. *Nature Review Neuroscience* 2: 387–396.

Clark RB, Mangoni ME, Lueger A, Couette B, Nargeot J, and Giles WR (2004) A rapidly activating delayed rectifier K+ current regulates pacemaker activity in adult mouse sinoatrial node cells. *American Journal of Physiology. Heart and Circulatory Physiology* 286: H1757–H1766.

Cooper PJ and Kohl P (2005) Species- and preparation-dependence of stretch effects on sino-atrial node pacemaking. *Annals of the New York Academy of Sciences* 1047: 324–335.

Cooper PJ, Lei M, Cheng LX, and Kohl P (2000) Selected contribution: Axial stretch increases spontaneous pacemaker activity in rabbit isolated sinoatrial node cells. *Journal of Applied Physiology* 89: 2099–2104.

Coppen SR, Kodama I, Boyett MR, Dobrzynski H, Takagishi Y, Honjo H, Yeh HI, and Severs NJ (1999) Connexin45, a major connexin of the rabbit sinoatrial node, is co-expressed with connexin43 in a restricted zone at the nodal-crista terminalis border. *The Journal of Histochemistry and Cytochemistry* 47: 907–918.

Craelius W, Chen V, and El-Sherif N (1988) Stretch activated ion channels in ventricular myocytes. *Bioscience Reports* 8: 407–414.

Csepe TA, Zhao J, Hansen BJ, Li N, Sul LV, Lim P, Wang Y, Simonetti OP, Kilic A, Mohler PJ, Janssen PM, and Fedorov VV (2016) Human sinoatrial node structure: 3D microanatomy of sinoatrial conduction pathways. *Progress in Biophysics and Molecular Biology* 120: 164–178.

Deck KA (1964) Dehnungseffekte am spontanschlagenden, isolierten Sinusknoten. *Pflügers Archiv für die Gesamte Physiologie des Menschen und der Tiere* 280: 120–130.

Demion M, Bois P, Launay P, and Guinamard R (2007) TRPM4, a Ca2+-activated nonselective cation channel in mouse sino-atrial node cells. *Cardiovascular Research* 73: 531–538.

Denyer JC and Brown HF (1990) Pacemaking in rabbit isolated sino-atrial node cells during Cs+block of the hyperpolarization-activated current if. *The Journal of Physiology* 429: 401–409.

Difrancesco D (1993) Pacemaker mechanisms in cardiac tissue. *Annual Review of Physiology* 55: 455–472.

Difrancesco D and Borer JS (2007) The funny current: Cellular basis for the control of heart rate. *Drugs* 67(Suppl 2): 15–24.

Difrancesco D, Ducouret P, and Robinson RB (1989) Muscarinic modulation of cardiac rate at low acetylcholine concentrations. *Science* 243: 669–671.

Difrancesco D and Tortora P (1991) Direct activation of cardiac pacemaker channels by intracellular cyclic AMP. *Nature* 351: 145–147.

Dobrzynski H, Anderson RH, Atkinson A, Borbas Z, D'Souza A, Fraser JF, Inada S, Logantha SJ, Monfredi O, Morris GM, Moorman AF, Nikolaidou T, Schneider H, Szuts V, Temple IP, Yanni J, and Boyett MR (2013) Structure, function and clinical relevance of the cardiac conduction system, including the atrioventricular ring and outflow tract tissues. *Pharmacology and Therapeutics* 139: 260–288.

Dobrzynski H, Boyett MR, and Anderson RH (2007) New insights into pacemaker activity: Promoting understanding of sick sinus syndrome. *Circulation* 115: 1921–1932.

Donald DE and Shepherd JT (1978) Reflexes from the heart and lungs: Physiological curiosities or important regulatory mechanisms. *Cardiovascular Research* 12: 446–469.

Efimov IR, Nikolski VP, Rothenberg F, Greener ID, Li J, Dobrzynski H, and Boyett M (2004) Structure–function relationship in the AV junction. *The Anatomical Record Part A: Discoveries in Molecular, Cellular, and Evolutionary Biology* 280: 952–965.

Egom E, Vella K, Hua R, Jansen HJ, Moghtadaei M, Polina I, Bogachev O, Hurnik R, Mackasey M, Rafferty S, Ray G, and Rose RA (2015) Impaired sinoatrial node function and increased susceptibility to atrial fibrillation in mice lacking natriuretic peptide receptor C. *Journal of Physiology* 593: 1127–1146.

Fedorov VV, Glukhov AV, and Chang R (2012) Conduction barriers and pathways of the sinoatrial pacemaker complex: Their role in normal rhythm and atrial arrhythmias. *American Journal of Physiology. Heart and Circulatory Physiology* 302: H1773–H1783.

Fedorov VV, Schuessler RB, Hemphill M, Ambrosi CM, Chang R, Voloshina AS, Brown K, Hucker WJ, and Efimov IR (2009) Structural and functional evidence for discrete exit pathways that connect the canine sinoatrial node and atria. *Circulation Research* 104: 915–923.

Fenske S, Krause SC, Hassan SI, Becirovic E, Auer F, Bernard R, Kupatt C, Lange P, ziegler T, Wotjak CT, Zhang H, Hammelmann V, Paparizos C, Biel M, and Wahl-Schott CA (2013) Sick sinus syndrome in HCN1-deficient mice. *Circulation* 128: 2585–2594.

Gaborit N, Le Bouter S, Szuts V, Varro A, Escande D, Nattel S, and Demolombe S (2007) Regional and tissue specific transcript signatures of ion channel genes in the non-diseased human heart. *The Journal of Physiology* 582: 675–693.

Gamble J, Taylor PB, and Kenno KA (1992) Myocardial stretch alters twitch characteristics and Ca^{2+} loading of sarcoplasmic reticulum in rat ventricular muscle. *Cardiovascular Research* 26: 865–870.

Gao Z, Singh MV, Hall DD, Koval OM, Luczak ED, Joiner ML, Chen B, Wu Y, Chaudhary AK, Martins JB, Hund TJ, Mohler PJ, Song LS, and Anderson ME (2011) Catecholamine-independent heart rate increases require Ca2+/calmodulin-dependent protein kinase II. *Circulation. Arrhythmia and Electrophysiology* 4: 379–387.

Garny A, Kohl P, Hunter PJ, Boyett MR, and Noble D (2003) One-dimensional rabbit sinoatrial node models: Benefits and limitations. *Journal of Cardiovascular Electrophysiology* 14: S121–S132.

Gehrmann J, Meister M, Maguire CT, Martins DC, Hammer PE, Neer EJ, Berul CI, and Mende U (2002) Impaired parasympathetic heart rate control in mice with a reduction of functional G protein betagamma-subunits. *American Journal of Physiology. Heart and Circulatory Physiology* 282: H445–H456.

Greener ID, Monfredi O, Inada S, Chandler NJ, Tellez JO, Atkinson A, Taube MA, Billeter R, Anderson RH, Efimov IR, Molenaar P, Sigg DC, Sharma V, Boyett MR, and Dobrzynski H (2011) Molecular architecture of the human specialised atrioventricular conduction axis. *Journal of Molecular and Cellular Cardiology* 50: 642–651.

Guharay F and Sachs F (1984) Stretch-activated single ion channel currents in tissue-cultured embryonic chick skeletal muscle. *The Journal of Physiology* 352: 685–701.

Han S, Wilson SJ, and Bolter CP (2010) Tertiapin-Q removes a mechanosensitive component of muscarinic control of the sinoatrial pacemaker in the rat. *Clinical and Experimental Pharmacology and Physiology* 37: 900–904.

Hancox JC, Levi AJ, and Brooksby P (1994) Intracellular calcium transients recorded with Fura-2 in spontaneously active myocytes isolated from the atrioventricular node of the rabbit heart. *Proceedings of the Biological Sciences* 255: 99–105.

Herrmann S, Stieber J, Stockl G, Hofmann F, and Ludwig A (2007) HCN4 provides a 'depolarization reserve' and is not required for heart rate acceleration in mice. *The EMBO Journal* 26: 4423–4432.

Hof T, Simard C, Rouet R, Salle L, and Guinamard R (2013) Implication of the TRPM4 nonselective cation channel in mammalian sinus rhythm. *Heart Rhythm* 10: 1683–1689.

Hoffman BF and Cranefield PF (1960) *Electrophysiology of the heart*. New York: McGraw-Hill.

Honjo H, Inada S, Lancaster MK, Yamamoto M, Niwa R, Jones SA, Shibata N, Mitsui K, Horiuchi T, Kamiya K, Kodama I, and Boyett MR (2003) Sarcoplasmic reticulum Ca2+ release is not a dominating factor in sinoatrial node pacemaker activity. *Circulation Research* 92: e41–e44.

Huang X, Du Y, Yang P, Lin S, Xi Y, Yang Z, and Ma A (2015) Age-dependent alterations of voltage-gated Na(+) channel isoforms in rat sinoatrial node. *Mechanisms of Ageing and Development* 152: 80–90.

Hucker WJ, Mccain ML, Laughner JI, Iaizzo PA, and Efimov IR (2008) Connexin 43 expression delineates two discrete pathways in the human atrioventricular junction. *The Anatomical Record* 291: 204–215.

Inada S, Zhang H, Tellez JO, Shibata N, Nakazawa K, Kamiya K, Kodama I, Mitsui K, Dobrzynski H, Boyett MR, and Honjo H (2014) Importance of gradients in membrane properties and electrical coupling in sinoatrial node pacing. *PLoS One* 9:e94565.

Inoue S and Becker AE (1998) Posterior extensions of the human compact atrioventricular node: A neglected anatomic feature of potential clinical significance. *Circulation* 97: 188–193.

Iribe G, Helmes M, and Kohl P (2007) Force-length relations in isolated intact cardiomyocytes subjected to dynamic changes in mechanical load. *American Journal of Physiology. Heart and Circulatory Physiology* 292: H1487–H1497.

Iribe G and Kohl P (2008) Axial stretch enhances sarcoplasmic reticulum Ca^{2+} leak and cellular Ca^{2+} reuptake in guinea pig ventricular myocytes: Experiments and models. *Progress in Biophysics and Molecular Biology* 97: 298–311.

Iribe G, Ward CW, Camelliti P, Bollensdorff C, Mason F, Burton RA, Garny A, Morphew MK, Hoenger A, Lederer WJ, and Kohl P (2009) Axial stretch of rat single ventricular cardiomyocytes causes an acute and transient increase in Ca^{2+} spark rate. *Circulation Research* 104: 787–795.

Irisawa H, Brown HF, and Giles W (1993) Cardiac pacemaking in the sinoatrial node. *Physiological Reviews* 73: 197–227.

Joyner RW and van Capelle FJ (1986) Propagation through electrically coupled cells. How a small SA node drives a large atrium. *Biophysical Journal* 50: 1157–1164.

Ju YK, Chu Y, Chaulet H, Lai D, Gervasio OL, Graham RM, Cannell MB, and Allen DG (2007) Store-operated Ca2+ influx and expression of TRPC genes in mouse sinoatrial node. *Circulation Research* 100: 1605–1614.

Ju YK, Liu J, Lee BH, Lai D, Woodcock EA, Lei M, Cannell MB, and Allen DG (2011) Distribution and functional role of inositol 1,4,5-trisphosphate receptors in mouse sinoatrial node. *Circulation Research* 109: 848–857.

Ju YK, Woodcock EA, Allen DG, and Cannell MB (2012) Inositol 1,4,5-trisphosphate receptors and pacemaker rhythms. *Journal of Molecular and Cellular Cardiology* 53: 375–381.

Kamiyama A, Niimura I, and Sugi H (1984) Length-dependent changes of pacemaker frequency in the isolated rabbit sinoatrial node. *The Japanese Journal of Physiology* 34: 153–165.

Kapoor N, Tran A, Kang J, Zhang R, Philipson KD, and Goldhaber JI (2015) Regulation of calcium clock-mediated pacemaking by inositol-1,4,5-trisphosphate receptors in mouse sinoatrial nodal cells. *The Journal of Physiology* 593: 2649–2663.

Keith A and Flack M (1907) The form and nature of the muscular connections between the primary divisions of the vertebrate heart. *Journal of Anatomy and Physiology* 41: 172–189.
Kodama I and Boyett MR (1985) Regional differences in the electrical activity of the rabbit sinus node. *Pflügers Archiv* 404: 214–226.
Kodama I, Boyett MR, Nikmaram MR, Yamamoto M, Honjo H, and Niwa R (1999) Regional differences in effects of E-4031 within the sinoatrial node. *The American Journal of Physiology* 276: H793–H802.
Kodama I, Nikmaram MR, Boyett MR, Suzuki R, Honjo H, and Owen JM (1997) Regional differences in the role of the Ca2+ and Na+currents in pacemaker activity in the sinoatrial node. *The American Journal of Physiology* 272: H2793–H2806.
Kohl P, Kamkin AG, Kiseleva IS, and Noble D (1994) Mechanosensitive fibroblasts in the sino-atrial node region of rat heart: Interaction with cardiomyocytes and possible role. *Experimental Physiology* 79: 943–956.
Kohl P and Noble D (1996) Mechanosensitive connective tissue: Potential influence on heart rhythm. *Cardiovascular Research* 32: 62–68.
Kreitner D (1985) Electrophysiological study of the two main pacemaker mechanisms in the rabbit sinus node. *Cardiovascular Research* 19: 304–318.
Krishnaswamy PS, Egom EE, Moghtadaei M, Jansen HJ, Azer J, Bogachev O, Mackasey M, Robbins C, and Rose RA (2015) Altered parasympathetic nervous system regulation of the sinoatrial node in Akita diabetic mice. *Journal of Molecular and Cellular Cardiology* 82: 125–135.
Kuhn M (2004) Molecular physiology of natriuretic peptide signalling. *Basic Research in Cardiology* 99: 76–82.
Kurian T, Ambrosi C, Hucker W, Fedorov VV, and Efimov IR (2010) Anatomy and electrophysiology of the human AV node. *Pacing and Clinical Electrophysiology* 33: 754–762.
Lai MH, Wu Y, Gao Z, Anderson ME, Dalziel JE, and Meredith AL (2014) BK channels regulate sinoatrial node firing rate and cardiac pacing in vivo. *American Journal of Physiology. Heart and Circulatory Physiology* 307: H1327–H1338.
Lakatta EG and Difrancesco D (2009) What keeps us ticking: A funny current, a calcium clock, or both? *Journal of Molecular and Cellular Cardiology* 47: 157–170.
Lakatta EG, Maltsev VA, and Vinogradova TM (2010) A coupled SYSTEM of intracellular Ca2+ clocks and surface membrane voltage clocks controls the timekeeping mechanism of the heart's pacemaker. *Circulation Research* 106: 659–673.
Lei M, Goddard C, Liu J, Leoni AL, Royer A, Fung SS, Xiao G, Ma A, Zhang H, Charpentier F, Vandenberg JI, Colledge WH, Grace AA, and Huang CL (2005) Sinus node dysfunction following targeted disruption of the murine cardiac sodium channel gene Scn5a. *The Journal of Physiology* 567: 387–400.
Lei M, Honjo H, Kodama I, and Boyett MR (2000) Characterisation of the transient outward K+ current in rabbit sinoatrial node cells. *Cardiovascular Research* 46: 433–441.
Lei M, Jones SA, Liu J, Lancaster MK, Fung SS, Dobrzynski H, Camelliti P, Maier SK, Noble D, and Boyett MR (2004) Requirement of neuronal- and cardiac-type sodium channels for murine sinoatrial node pacemaking. *The Journal of Physiology* 559: 835–848.
Lei M, Zhang H, Grace AA, and Huang CL (2007) SCN5A and sinoatrial node pacemaker function. *Cardiovascular Research* 74: 356–365.
Li J, Qu J, and Nathan RD (1997) Ionic basis of ryanodine's negative chronotropic effect on pacemaker cells isolated from the sinoatrial node. *The American Journal of Physiology* 273: H2481–H2489.
Li N, Csepe TA, Hansen BJ, Dobrzynski H, Higgins RS, Kilic A, Mohler PJ, Janssen PM, Rosen MR, Biesiadecki BJ, and Fedorov VV (2015) Molecular mapping of sinoatrial node HCN channel expression in the human heart. *Circulation. Arrhythmia and Electrophysiology* 8: 1219–1227.
Liao Z, Lockhead D, Larson ED, and Proenza C (2010) Phosphorylation and modulation of hyperpolarization-activated HCN4 channels by protein kinase A in the mouse sinoatrial node. *The Journal of General Physiology* 136: 247–258.
Lin W, Laitko U, Juranka PF, and Morris CE (2007) Dual stretch responses of mHCN2 pacemaker channels: Accelerated activation, accelerated deactivation. *Biophysical Journal* 92: 1559–1572.
Little SC and Mohler PJ (2013) TRPM4 modulates sinus node diastolic depolarization. *Heart Rhythm* 10: 1690–1691.
Liu J, Dobrzynski H, Yanni J, Boyett MR, and Lei M (2007) Organisation of the mouse sinoatrial node: Structure and expression of HCN channels. *Cardiovascular Research* 73: 729–738.
Lonardo G, Cerbai E, Casini S, Giunti G, Bonacchi M, Battaglia F, Fiorani B, Stefano PL, Sani G, and Mugelli A (2004) Atrial natriuretic peptide modulates the hyperpolarization-activated current (If) in human atrial myocytes. *Cardiovascular Research* 63: 528–536.
Lucas KA, Pitari GM, Kazerounian S, Ruiz-Stewart I, Park J, Schulz S, Chepenik KP, and Waldman SA (2000) Guanylyl cyclases and signaling by cyclic GMP. *Pharmacological Reviews* 52: 375–414.
Ludwig A, Budde T, Stieber J, Moosmang S, Wahl C, Holthoff K, Langebartels A, Wotjak C, Munsch T, Zong X, Feil S, Feil R, Lancel M, Chien KR, Konnerth A, Pape HC, Biel M, and Hofmann F (2003) Absence epilepsy and sinus dysrhythmia in mice lacking the pacemaker channel HCN2. *The EMBO Journal* 22: 216–224.
Lyashkov AE, Vinogradova TM, Zahanich I, Li Y, Younes A, Nuss HB, Spurgeon HA, Maltsev VA, and Lakatta EG (2009) Cholinergic receptor signaling modulates spontaneous firing of sinoatrial nodal cells via integrated effects on PKA-dependent Ca(2+) cycling and I(KACh). *American Journal of Physiology. Heart and Circulatory Physiology* 297: H949–H959.
Lyford GL, Strege PR, Shepard A, Ou Y, Ermilov L, Miller SM, Gibbons SJ, Rae JL, Szurszewski JH, and Farrugia G (2002) α_{1C} ($Ca_V1.2$) L-type calcium channel mediates mechanosensitive calcium regulation. *American Journal of Physiology. Cell Physiology* 283: C1001–C1008.
Maier SK, Westenbroek RE, Yamanushi TT, Dobrzynski H, Boyett MR, Catterall WA, and Scheuer T (2003) An unexpected requirement for brain-type sodium channels for control of heart rate in the mouse sinoatrial node. *Proceedings of the National Academy of Sciences of the United States of America* 100: 3507–3512.
Mangoni ME, Couette B, Bourinet E, Platzer J, Reimer D, Striessnig J, and Nargeot J (2003) Functional role of L-type Cav1.3 Ca2+ channels in cardiac pacemaker activity. *Proceedings of the National Academy of Sciences of the United States of America* 100: 5543–5548.
Mangoni ME, Couette B, Marger L, Bourinet E, Striessnig J, and Nargeot J (2006a) Voltage-dependent calcium channels and cardiac pacemaker activity: From ionic currents to genes. *Progress in Biophysics and Molecular Biology* 90: 38–63.
Mangoni ME and Nargeot J (2001) Properties of the hyperpolarization-activated current (I(f)) in isolated mouse sino-atrial cells. *Cardiovascular Research* 52: 51–64.
Mangoni ME and Nargeot J (2008) Genesis and regulation of the heart automaticity. *Physiological Reviews* 88: 919–982.
Mangoni ME, Traboulsie A, Leoni AL, Couette B, Marger L, Le Quang K, Kupfer E, Cohen-Solal A, Vilar J, Shin HS, Escande D, Charpentier F, Nargeot J, and Lory P (2006b) Bradycardia and slowing of the atrioventricular conduction in mice lacking CaV3.1/alpha1G T-type calcium channels. *Circulation Research* 98: 1422–1430.
Mani BC and Pavri BB (2014) Dual atrioventricular nodal pathways physiology: A review of relevant anatomy, electrophysiology, and electrocardiographic manifestations. *Indian Pacing and Electrophysiology Journal* 14: 12–25.
Marger L, Mesirca P, Alig J, Torrente A, Dubel S, Engeland B, Kanani S, Fontanaud P, Striessnig J, Shin HS, Isbrandt D, Ehmke H, Nargeot J, and Mangoni ME (2011a) Functional roles of Ca(v)1.3, Ca(v)3.1 and HCN channels in automaticity of mouse atrioventricular cells: Insights into the atrioventricular pacemaker mechanism. *Channels (Austin, Tex.)* 5: 251–261.
Marger L, Mesirca P, Alig J, Torrente A, Dubel S, Engeland B, Kanani S, Fontanaud P, Striessnig J, Shin HS, Isbrandt D, Ehmke H, Nargeot J, and Mangoni ME (2011b) Pacemaker activity and ionic currents in mouse atrioventricular node cells. *Channels (Austin, Tex.)* 5: 241–250.
Marionneau C, Couette B, Liu J, Li H, Mangoni ME, Nargeot J, Lei M, Escande D, and Demolombe S (2005) Specific pattern of ionic channel gene expression associated with pacemaker activity in the mouse heart. *The Journal of Physiology* 562: 223–234.
Meijler FL and Janse MJ (1988) Morphology and electrophysiology of the mammalian atrioventricular node. *Physiological Reviews* 68: 608–647.
Mesirca P, Bidaud I, Briec F, Evain S, Torrente AG, Le Quang K, Leoni AL, Baudot M, Marger L, Chung You Chong A, Nargeot J, Striessnig J, Wickman K, Charpentier F, and Mangoni ME (2016a) G protein-gated IKACh channels as therapeutic targets for treatment of sick sinus syndrome and heart block. *Proceedings of the National Academy of Sciences of the United States of America* 113: E932–E941.
Mesirca P, Bidaud I, and Mangoni ME (2016b) Rescuing cardiac automaticity in L-type Cav1.3 channelopathies and beyond. *The Journal of Physiology* 594: 5869–5879.
Mesirca P, Torrente AG, and Mangoni ME (2014) T-type channels in the sino-atrial and atrioventricular pacemaker mechanism. *Pflügers Archiv* 466: 791–799.
Mitsuiye T, Shinagawa Y, and Noma A (2000) Sustained inward current during pacemaker depolarization in mammalian sinoatrial node cells. *Circulation Research* 87: 88–91.

Moghtadaei M, Jansen HJ, Mackasey M, Rafferty SA, Bogachev O, Sapp JL, Howlett SE, and Rose RA (2016a) The impacts of age and frailty on heart rate and sinoatrial node function. *The Journal of Physiology* 594: 7105–7126.
Moghtadaei M, Polina I, and Rose RA (2016b) Electrophysiological effects of natriuretic peptides in the heart are mediated by multiple receptor subtypes. *Progress in Biophysics and Molecular Biology* 120: 37–49.
Monfredi O, Dobrzynski H, Mondal T, Boyett MR, and Morris GM (2010) The anatomy and physiology of the sinoatrial node—A contemporary review. *Pacing and Clinical Electrophysiology* 33: 1392–1406.
Morris CE (2011) Pacemaker, potassium, calcium, sodium: Stretch modulation of the volatge-gated channels. In: Kohl P, Sachs F, and Franz MR (eds.) *Cardiac Mechano-Electric Coupling and Arrhythmias*, 2nd edn. Oxford: Oxford University Press.
Munk AA, Adjemian RA, Zhao J, Ogbaghebriel A, and Shrier A (1996) Electrophysiological properties of morphologically distinct cells isolated from the rabbit atrioventricular node. *The Journal of Physiology* 493(Pt 3): 801–818.
Nerbonne JM and Kass RS (2005) Molecular physiology of cardiac repolarization. *Physiological Reviews* 85: 1205–1253.
Nikmaram MR, Boyett MR, Kodama I, Suzuki R, and Honjo H (1997) Variation in effects of Cs^+, UL-FS-49, and ZD-7288 within sinoatrial node. *The American Journal of Physiology* 272: H2782–H2792.
Nikolaidou T, Aslanidi OV, Zhang H, and Efimov IR (2012) Structure–function relationship in the sinus and atrioventricular nodes. *Pediatric Cardiology* 33: 890–899.
Ono K and Ito H (1995) Role of rapidly activating delayed rectifier K+ current in sinoatrial node pacemaker activity. *The American Journal of Physiology* 269: H453–H462.
Ono K, Shibata S, and Iijima T (2000) Properties of the delayed rectifier potassium current in porcine sino-atrial node cells. *The Journal of Physiology* 524(Pt 1): 51–62.
Opthof T (1988) The mammalian sinoatrial node. *Cardiovascular Drugs and Therapy* 1: 573–597.
Pathak CL (1973) Autoregulation of chronotropic response of the heart through pacemaker stretch. *Cardiology* 58: 45–64.
Pauza DH, Rysevaite K, Inokaitis H, Jokubauskas M, Pauza AG, Brack KE, and Pauziene N (2014) Innervation of sinoatrial nodal cardiomyocytes in mouse. A combined approach using immunofluorescent and electron microscopy. *Journal of Molecular and Cellular Cardiology* 75: 188–197.
Pauza DH, Saburkina I, Rysevaite K, Inokaitis H, Jokubauskas M, Jalife J, and Pauziene N (2013) Neuroanatomy of the murine cardiac conduction system: A combined stereomicroscopic and fluorescence immunohistochemical study. *Autonomic Neuroscience* 176: 32–47.
Potter LR, Abbey-Hosch S, and Dickey DM (2006) Natriuretic peptides, their receptors, and cyclic guanosine monophosphate-dependent signaling functions. *Endocrine Reviews* 27: 47–72.
Prosser BL, Ward CW, and Lederer WJ (2011) X-ROS signaling: Rapid mechano-chemo transduction in heart. *Science* 333: 1440–1445.
Prosser BL, Ward CW, and Lederer WJ (2013) X-ROS signalling is enhanced and graded by cyclic cardiomyocyte stretch. *Cardiovascular Research* 98: 307–314.
Quinn TA, Camelliti P, Rog-Zielinska EA, Siedlecka U, Poggioli T, O'toole ET, Knopfel T, and Kohl P (2016) Electrotonic coupling of excitable and nonexcitable cells in the heart revealed by optogenetics. *Proceedings of the National Academy of Sciences of the United States of America* 113: 14852–14857.
Quinn TA and Kohl P (2012) Mechano-sensitivity of cardiac pacemaker function: Pathophysiological relevance, experimental implications, and conceptual integration with other mechanisms of rhythmicity. *Progress in Biophysics and Molecular Biology* 110: 257–268.
Rajala GM, Pinter MJ, and Kaplan S (1977) Response of the quiescent heart tube to mechanical stretch in the intact chick embryo. *Developmental Biology* 61: 330–337.
Ridley JM, Cheng H, Harrison OJ, Jones SK, Smith GL, Hancox JC, and Orchard CH (2008) Spontaneous frequency of rabbit atrioventricular node myocytes depends on SR function. *Cell Calcium* 44: 580–591.
Rigg L and Terrar DA (1996) Possible role of calcium release from the sarcoplasmic reticulum in pacemaking in guinea-pig sino-atrial node. *Experimental Physiology* 81: 877–880.
Rose RA and Giles WR (2008) Natriuretic peptide C receptor signalling in the heart and vasculature. *The Journal of Physiology* 586: 353–366.
Rose RA, Hatano N, Ohya S, Imaizumi Y, and Giles WR (2007) C-type natriuretic peptide activates a non-selective cation current in acutely isolated rat cardiac fibroblasts via natriuretic peptide C receptor-mediated signalling. *The Journal of Physiology* 580: 255–274.
Rose RA, Lomax AE, Kondo CS, Anand-Srivastava MB, and Giles WR (2004) Effects of C-type natriuretic peptide on ionic currents in mouse sinoatrial node: a role for the NPR-C receptor. *American Journal of Physiology. Heart and Circulatory Physiology* 286: H1970–H1977.
Rosen MR, Robinson RB, Brink PR, and Cohen IS (2011) The road to biological pacing. *Nature Reviews Cardiology* 8: 656–666.
Rubenstein DS and Lipsius SL (1989) Mechanisms of automaticity in subsidiary pacemakers from cat right atrium. *Circulation Research* 64: 648–657.
Sah R, Mesirca P, Van den Boogert M, Rosen J, Mably J, Mangoni ME, and Clapham DE (2013) Ion channel-kinase TRPM7 is required for maintaining cardiac automaticity. *Proceedings of the National Academy of Sciences of the United States of America* 110: E3037–E3046.
Schmitt N, Grunnet M, and Olesen SP (2014) Cardiac potassium channel subtypes: New roles in repolarization and arrhythmia. *Physiological Reviews* 94: 609–653.
Shi W, Wymore R, Yu H, Wu J, Wymore RT, Pan Z, Robinson RB, Dixon JE, Mckinnon D, and Cohen IS (1999) Distribution and prevalence of hyperpolarization-activated cation channel (HCN) mRNA expression in cardiac tissues. *Circulation Research* 85: e1–e6.
Shinagawa Y, Satoh H, and Noma A (2000) The sustained inward current and inward rectifier K+ current in pacemaker cells dissociated from rat sinoatrial node. *The Journal of Physiology* 523(Pt 3): 593–605.
Springer J, Azer J, Hua R, Robbins C, Adamczyk A, Mcboyle S, Bissell MB, and Rose RA (2012) The natriuretic peptides BNP and CNP increase heart rate and electrical conduction by stimulating ionic currents in the sinoatrial node and atrial myocardium following activation of guanylyl cyclase-linked natriuretic peptide receptors. *Journal of Molecular and Cellular Cardiology* 52: 1122–1134.
Stieber J, Herrmann S, Feil S, Loster J, Feil R, Biel M, Hofmann F, and Ludwig A (2003) The hyperpolarization-activated channel HCN4 is required for the generation of pacemaker action potentials in the embryonic heart. *Proceedings of the National Academy of Sciences of the United States of America* 100: 15235–15240.
Stockbridge LL and French AS (1988) Stretch-activated cation channels in human fibroblasts. *Biophysical Journal* 54: 187–190.
Tawara S (2000) *The conduction system of the mammalian heart*. London: Imperial College Press.
Temple IP, Inada S, Dobrzynski H, and Boyett MR (2013) Connexins and the atrioventricular node. *Heart Rhythm* 10: 297–304.
Torrente AG, Mesirca P, Neco P, Rizzetto R, Dubel S, Barrere C, Sinegger-Brauns M, Striessnig J, Richard S, Nargeot J, Gomez AM, and Mangoni ME (2016) L-type Cav1.3 channels regulate ryanodine receptor-dependent Ca2+ release during sino-atrial node pacemaker activity. *Cardiovascular Research* 109: 451–461.
Toyoda F, Ding WG, and Matsuura H (2005) Responses of the sustained inward current to autonomic agonists in guinea-pig sino-atrial node pacemaker cells. *British Journal of Pharmacology* 144: 660–668.
Uese K, Hagiwara N, Miyawaki T, and Kasanuki H (1999) Properties of the transient outward current in rabbit sino-atrial node cells. *Journal of Molecular and Cellular Cardiology* 31: 1975–1984.
Unudurthi SD, Wu X, Qian L, Amari F, Onal B, Li N, Makara MA, Smith SA, Snyder J, Fedorov VV, Coppola V, Anderson ME, Mohler PJ, and Hund TJ (2016) Two-pore K+ channel TREK-1 regulates sinoatrial node membrane excitability. *Journal of the American Heart Association* 5:e002865.
van Borren MM, Verkerk AO, Wilders R, Hajji N, Zegers JG, Bourier J, Tan HL, Verheijck EE, Peters SL, Alewijnse AE, and Ravesloot JH (2010) Effects of muscarinic receptor stimulation on Ca2+ transient, cAMP production and pacemaker frequency of rabbit sinoatrial node cells. *Basic Research in Cardiology* 105: 73–87.
van Weerd JH and Christoffels VM (2016) The formation and function of the cardiac conduction system. *Development* 143: 197–210.
Vedantham V (2015) New approaches to biological pacemakers: Links to sinoatrial node development. *Trends in Molecular Medicine* 21: 749–761.
Verheijck EE, van Ginneken AC, Bourier J, and Bouman LN (1995) Effects of delayed rectifier current blockade by E-4031 on impulse generation in single sinoatrial nodal myocytes of the rabbit. *Circulation Research* 76: 607–615.
Verheijck EE, van Kempen MJ, Veereschild M, Lurvink J, Jongsma HJ, and Bouman LN (2001) Electrophysiological features of the mouse sinoatrial node in relation to connexin distribution. *Cardiovascular Research* 52: 40–50.

Verkerk AO, Wilders R, van Borren MM, Peters RJ, Broekhuis E, Lam K, Coronel R, De Bakker JM, and TAN HL (2007) Pacemaker current (I(f)) in the human sinoatrial node. *European Heart Journal* 28: 2472–2478.
Vinogradova TM, Bogdanov KY, and Lakatta EG (2002) beta-Adrenergic stimulation modulates ryanodine receptor Ca(2+) release during diastolic depolarization to accelerate pacemaker activity in rabbit sinoatrial nodal cells. *Circulation Research* 90: 73–79.
Vinogradova TM, Fedorov VV, Yuzyuk TN, Zaitsev AV, and Rosenshtraukh LV (1998) Local cholinergic suppression of pacemaker activity in the rabbit sinoatrial node. *Journal of Cardiovascular Pharmacology* 32: 413–424.
Vinogradova TM, Lyashkov AE, Zhu W, Ruknudin AM, Sirenko S, Yang D, Deo S, Barlow M, Johnson S, Caffrey JL, Zhou YY, Xiao RP, Cheng H, Stern MD, Maltsev VA, and Lakatta EG (2006) High basal protein kinase A-dependent phosphorylation drives rhythmic internal Ca2+ store oscillations and spontaneous beating of cardiac pacemaker cells. *Circulation Research* 98: 505–514.
Vinogradova TM, Sirenko S, Lyashkov AE, Younes A, Li Y, Zhu W, Yang D, Ruknudin AM, Spurgeon H, and Lakatta EG (2008) Constitutive phosphodiesterase activity restricts spontaneous beating rate of cardiac pacemaker cells by suppressing local Ca2+ releases. *Circulation Research* 102: 761–769.
Wainger BJ, Degennaro M, Santoro B, Siegelbaum SA, and Tibbs GR (2001) Molecular mechanism of cAMP modulation of HCN pacemaker channels. *Nature* 411: 805–810.
Weisbrod D, Khun SH, Bueno H, Peretz A, and Attali B (2016) Mechanisms underlying the cardiac pacemaker: The role of SK4 calcium-activated potassium channels. *Acta Pharmacologica Sinica* 37: 82–97.
Wickman K, Nemec J, Gendler SJ, and Clapham DE (1998) Abnormal heart rate regulation in GIRK4 knockout mice. *Neuron* 20: 103–114.
Wiedmann F, Schmidt C, Lugenbiel P, Staudacher I, Rahm AK, Seyler C, Schweizer PA, Katus HA, and Thomas D (2016) Therapeutic targeting of two-pore-domain potassium (K(2P)) channels in the cardiovascular system. *Clinical Science (London)* 130: 643–650.
Wilson SJ and Bolter CP (2001) Interaction of the autonomic nervous system with intrinsic cardiac rate regulation in the guinea-pig, Cavia porcellus. *Comparative Biochemistry and Physiology. Part A, Molecular & Integrative Physiology* 130: 723–730.
Wilson SJ and Bolter CP (2002) Do cardiac neurons play a role in the intrinsic control of heart rate in the rat? *Experimental Physiology* 87: 675–682.
Yamamoto M, Honjo H, Niwa R, and Kodama I (1998) Low-frequency extracellular potentials recorded from the sinoatrial node. *Cardiovascular Research* 39: 360–372.
Yaniv Y, Spurgeon HA, Lyashkov AE, Yang D, Ziman BD, Maltsev VA, and Lakatta EG (2012) Crosstalk between mitochondrial and sarcoplasmic reticulum Ca2+ cycling modulates cardiac pacemaker cell automaticity. *PLoS One* 7:e37582.
Yuill KH and Hancox JC (2002) Characteristics of single cells isolated from the atrioventricular node of the adult guinea-pig heart. *Pflügers Archiv* 445: 311–320.
Zaza A, Robinson RB, and Difrancesco D (1996) Basal responses of the L-type Ca2+ and hyperpolarization-activated currents to autonomic agonists in the rabbit sino-atrial node. *The Journal of Physiology* 491(Pt 2): 347–355.
Zhang H, Holden AV, and Boyett MR (2002) Sustained inward current and pacemaker activity of mammalian sinoatrial node. *Journal of Cardiovascular Electrophysiology* 13: 809–812.
Zhang Q, Timofeyev V, Lu L, Li N, Singapuri A, Long MK, Bond CT, Adelman JP, and Chiamvimonvat N (2008) Functional roles of a Ca2+-activated K+ channel in atrioventricular nodes. *Circulation Research* 102: 465–471.
Zicha S, Fernandez-Velasco M, Lonardo G, L'Heureux N, and Nattel S (2005) Sinus node dysfunction and hyperpolarization-activated (HCN) channel subunit remodeling in a canine heart failure model. *Cardiovascular Research* 66: 472–481.

Further Reading

Atkinson AJ, Logantha SJ, Hao G, Yanni J, Fedorenko O, Sinha A, Gilbert SH, Benson AP, Buckley DL, Anderson RH, Boyett MR, and Dobrzynski H (2013) Functional, anatomical, and molecular investigation of the cardiac conduction system and arrhythmogenic atrioventricular ring tissue in the rat heart. *Journal of the American Heart Association* 2:e000246.
Boyett MR (2009) 'And the beat goes on'. The cardiac conduction system: the wiring system of the heart. *Experimental Physiology* 94: 1035–1049.